Electronic Supplementary Material (ESI) for ChemComm.
This journal is © The Royal Society of Chemistry 2019

ELECTRONIC SUPPLEMENTARY INFORMATION

An efficient dynamic asymmetric catalytic system within a zinc-templated network

.

Anna Serra-Pont, Ignacio Alfonso, Jordi Solà,* Ciril Jimeno.*

Institute of Advanced Chemistry of Catalonia (IQAC-CSIC)

Jordi Girona 18-26, E08034 Barcelona (Spain)

TABLE OF CONTENTS

1. Experimental section

All the reagents and solvents were purchased from commercial suppliers and used without further purification. Anhydrous solvents were obtained from a Solvent Purification System. TLC was performed on silica gel 60 F_{254} Aluminium sheets. Flash chromatography was performed using silica gel P60 (200-500 mesh). Room temperature (rt) refers to 25°C. HPLC analyses were performed using modular equipment with autosampler and UV-Vis detector. NMR spectra were recorded on an automated Varian Mercury 400 instrument (400 MHz for ^{1}H, 101 MHz for ^{13}C and 376 MHz for ^{19}F). The chemical shifts are reported in ppm and referenced to the appropriate NMR solvent peak, and coupling constants (J) are reported in Hertz (Hz). Proton signal multiplicities are indicated by: s (singlet), d (doublet), t (triplet), q (quartet), m (multiplet), b (broad) or a combination of them. High resolution Mass Spectrometry analyses were acquired by ESI-TOF. Mass Spectrometry analyses of complexes were performed using a MALDI TOF/TOF mass spectrometer. Optical rotations were measured on a Perkin elmer 341 polarimeter using a 1 mL cell with a 1 dm path length at room temperature using the sodium D line as wavelength, and a suitable solvent that is reported along with the concentration (c=g/100ml). Absorbance measurements were performed on a Molecular Devices SpectraMax M5, at room temperature. UV-Vis spectra were recorded in THF using a quartz cell. For all the experiments, the observed spectral region was from 200 to 500 nm. For the determination of formation constants, the spectrophotometric data were fitted with the HypSpec software. The distribution diagrams of species were calculated using the software Hyperquad Simulation and Speciation (HySS).

2. Synthesis of ligands

2.1. 5-Nitro-2,2'-bipyridine

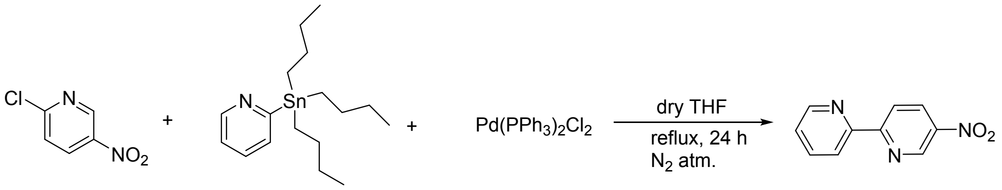

Adapted from a previously described procedure.[1] A solution of 2-chloro-5-nitropyridine (801 mg, 5.05 mmol), 2-tributylstannylpyridine (2 g, 5.5 mmol, 1.1 equiv.), and $Pd(PPh_3)_2Cl_2$ (168 mg, 0.24 mmol, 0.05 equiv.) in dry THF (8 mL) was refluxed for 24 h under nitrogen atmosphere. During the course of the reaction, the color changed from yellow to black as Pd(0) was formed. The reaction mixture was cooled, diluted with ether, filtered through a silica gel-celite bed and eluted with DCM. Evaporation of the solvent gave a yellow colored solid. The crude product was purified by silica gel chromatography eluting with DCM. 5-Nitro-2,2'-bipyridine was obtained as a pale yellow solid (610 mg, 3.03 mmol, 60%).

^{1}H NMR (400 MHz, $CDCl_3$) δ (ppm) 9.47 (dd, *J* = 2.6, 0.8 Hz, 1H), 8.73 (ddd, *J* = 4.8, 1.8, 0.9 Hz, 1H), 8.65 (dd, *J* = 8.8, 0.8 Hz, 1H), 8.57 (dd, *J* = 8.8, 2.6 Hz, 1H), 8.51 (dt, *J* = 8.0, 1.1 Hz, 1H), 7.88 (ddd, *J* = 8.1, 7.6, 1.8 Hz, 1H), 7.41 (ddd, *J* = 7.5, 4.7, 1.2 Hz, 1H).
^{13}C NMR (101 MHz, $CDCl_3$) δ (ppm) 161.0 (C), 153.9 (C), 149.7 (CH), 144.9 (CH), 144.2 (C), 137.4 (CH), 132.1 (CH), 125.3 (CH), 122.6 (CH), 121.2 (CH).
HRMS (ESI-TOF) calcd. For $C_{10}H_8N_3O_2$ $[M+H]^+$ (m/z): 202.0617, found: 202.0624.

2.2. 5-Amino-2,2'-bipyridine

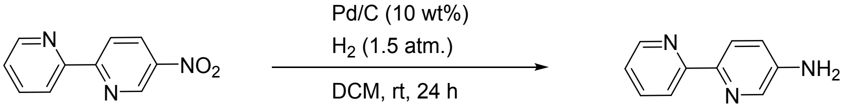

5-Nitro-2,2'-bipyridine (785 mg, 3.9 mmol) was dissolved in DCM (29 mL) under nitrogen. After addition of 10 % Pd/C (78.5 mg) catalyst, the reaction mixture was stirred at rt for 24 h under hydrogen atmosphere. After this time, catalyst was removed by filtration through celite, and the solvent was evaporated to afford 5-amino-2,2'-bipyridine (614 mg, 3.59 mmol, 92%) as a pale yellow solid.

^{1}H NMR (400 MHz, $CDCl_3$) δ (ppm) 8.61 (d, J = 4.9 Hz, 1H), 8.24 (d, J = 8.1 Hz, 1H), 8.19 (d, J = 8.5 Hz, 1H), 8.15 (d, J = 2.8 Hz, 1H), 7.74 (td, J = 7.7, 1.8 Hz, 1H), 7.20 (ddd, J = 7.5, 4.8, 1.1 Hz, 1H), 7.08 (dd, J = 8.5, 2.9 Hz, 1H), 3.86 (bs, 2H, $N\underline{H_2}$).
^{13}C NMR (101 MHz, $CDCl_3$) δ (ppm) 156.6 (C), 149.1 (CH), 147.1 (C), 142.9 (C), 136.8 (CH), 136.6 (CH), 122.6 (CH), 122.2 (CH), 121.8 (CH), 120.0 (CH).
HRMS (ESI-TOF) calcd. For $C_{10}H_{10}N_3$ $[M+H]^+$ (m/z): 172.0875, found: 172.0875.

2.3. *tert*-butyl (*S*)-2-([2,2'-bipyridin]-5-ylcarbamoyl)pyrrolidine-1-carboxylate

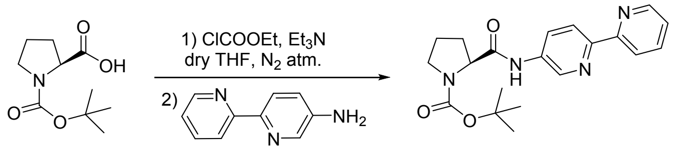

To a solution of the Boc-*L*-proline (400 mg, 1.86 mmol, 1 equiv.) in dry THF (6 mL), was added Et_3N (259 µL, 1.86 mmol, 1 equiv.) under nitrogen atmosphere at 0°C. Then, ethylchloroformate (177 µL, 1.86 mmol, 1 equiv.) was added dropwise and the reaction mixture was stirred for 30 min at 0 °C. After that, 5-amino-2,2'-bipyridine (346 mg, 1.86 mmol, 1 equiv.) was added and the resulting reaction was stirred at 0°C for 1 h, at room temperature for 2h and at 70°C for 24 h. After cooled down to room temperature, the mixture was diluted with EtOAc, filtered and the solvent was evaporated. The crude was purified by silica gel flash-column chromatography using a gradient of Hexane/EtOAc + 1% Et_3N as eluent to give *tert*-

butyl (*S*)-2-([2,2’-bipyridin]-5-ylcarbamoyl)pyrrolidine-1-carboxylate (490 mg, 1.33 mmol, 71%) as a white solid.

^{1}H NMR (400 MHz, $CDCl_3$, rotamers) δ (ppm) 9.93 (bs, 1H), 8.63 (m, 2H), 8.28 (m, 2H), 8.20 (m, 1H), 7.76 (t, J = 7.8 Hz, 1H), 7.28 – 7.20 (m, 1H), 4.52 (bs, 1H), 3.63 – 3.19 (m, 2H), 2.54 (bs, 1H), 2.06 – 1.75 (m, 3H), 1.51 (s, 9H).
^{13}C NMR (101 MHz, $CDCl_3$) δ (ppm) 170.6 (C), 156.9 (C), 155.9 (C), 151.5 (C), 149.2 (CH), 140.4 (CH), 136.9 (CH), 135.6 (C), 127.1 (CH), 123.2 (CH), 121.2 (CH), 120.6 (CH), 81.4 (C), 60.6 (CH), 47.5 (CH_2), 28.6 (3 x CH_3), 27.2 (CH_2), 24.8 (CH_2).
HRMS (ESI-TOF) calcd. For $C_{20}H_{25}N_4O_3$ $[M+H]^+$ (m/z): 369.1927, found: 369.2203.
$[\alpha]^{20}_D$ = -98.8 (c = 1.0, $CHCl_3$).

2.4. (*S*)-*N*-([2,2’-bipyridin]-5-yl)pyrrolidine-2-carboxamide (bipyPro)

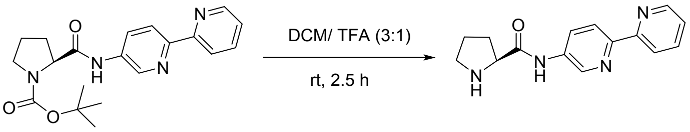

tert-butyl (*S*)-2-([2,2’-bipyridin]-5-ylcarbamoyl)pyrrolidine-1-carboxylate (200 mg, 0.54 mmol) was dissolved in a mixture of DCM (6 mL) and trifluoroacetic acid (2 mL) and stirred at room temperature for 2 h. The resulting reaction mixture was concentrated under reduced pressure and saturated aqueous sodium bicarbonate was added slowly to the reaction residue to make it weakly alkaline. The solution thus obtained was extracted with a mixture of chloroform/2-propanol 3:1 (2 x 10 mL). The combined organic extracts were dried over anhydrous $MgSO_4$ and the solvent was removed with a rotary evaporator. If necessary, the crude product was purified by flash chromatography using DCM/ammonium solution 7 N in MeOH to afford (*S*)-*N*-([2,2’-bipyridin]-5-yl)pyrrolidine-2-carboxamide (132 mg, 0.49 mmol, 90%) as a white solid.

^{1}H NMR (400 MHz, $CDCl_3$) δ (ppm) 9.97 (bs, 1H), 8.74 (dd, J = 2.5, 0.8 Hz, 1H), 8.64 (ddd, J = 4.8, 1.8, 0.9 Hz, 1H), 8.38 – 8.26 (m, 3H), 7.78 (td, J = 7.8, 1.8 Hz, 1H), 7.26 (m, 1H), 3.90 (dd, J = 9.3, 5.2 Hz, 1H), 3.06 (m, 2H), 2.30 (bs, 1H), 2.26 – 2.17 (m, 1H), 2.06 (m, 1H), 1.79 (m, 2H).
^{13}C NMR (101 MHz, $CDCl_3$) δ (ppm) 174.1 (C=O), 156.0 (C), 151.6 (C), 149.3 (CH), 140.3 (CH), 137.0 (CH), 135.0 (C), 127.0 (CH), 123.4 (CH), 121.4 (CH), 120.8 (CH), 61.1 (CH), 47.5 (CH_2), 30.9 (CH_2), 26.5 (CH_2).
HRMS (ESI-TOF) calcd. For $C_{15}H_{17}N_4O$ $[M+H]^+$ (m/z): 269.1402, found: 269.1508.

$[\alpha]^{20}_D$ = -47.3 (c = 1.0, $CHCl_3$).

2.5. 1-([2,2'-bipyridin]-5-yl)-3-(3,5-bis(trifluoromethyl)phenyl)thiourea (bipyTU)

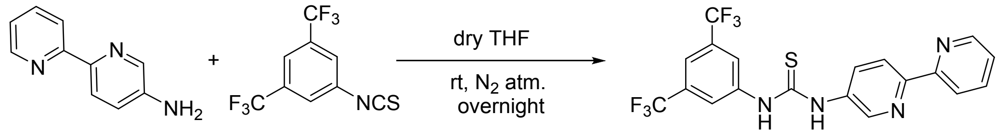

To a solution of 5-amino-2,2'-bipyridine (300 mg, 1.75 mmol) in dry THF (3 mL) under nitrogen atmosphere, 3,5-bis(trifluoromethyl)phenyl isothiocyanate (329 µL, 1.8 mmol) was added at 0°C. The mixture was stirred overnight at room temperature. Then, the solvent was evaporated. If necessary, the crude product was purified by flash chromatography using DCM/MeOH + 1% Et_3N as a eluent to give 1-([2,2'-bipyridin]-5-yl)-3-(3,5-bis(trifluoromethyl)phenyl)thiourea (542 mg, 1.22 mmol, 70%) as a pale yellow solid.

^{1}H NMR (400 MHz, CD_3OD) δ (ppm) 8.78 (d, J = 2.5 Hz, 1H), 8.65 (m, 1H), 8.33 (m, 1H), 8.31 (m, 1H), 8.23 (s, 2H), 8.18 (dd, J = 8.6, 2.6 Hz, 1H), 7.94 (td, J = 7.8, 1.8 Hz, 1H), 7.70 (s, 1H), 7.43 (ddd, J = 7.5, 4.9, 1.2 Hz, 1H).
^{19}F NMR (376 MHz, CD_3OD) δ (ppm) -64.6.
^{13}C NMR (101 MHz, CD_3OD) δ (ppm) 182.7 (C=S), 156.7 (C), 153.5 (C), 150.2 (CH), 145.9 (CH), 142.9 (C), 138.7 (CH), 137.8 (C), 133.6 (CH), 132.6 (q, $^2J_{CF}$ = 33 Hz, 2C), 125.1 (C), 124.8 (bq, 2CH), 123.4 (q, $^1J_{CF}$ = 273 Hz, $2CF_3$), 122.5 (CH), 122.2 (CH), 118.7 (m, CH).
HRMS (ESI-TOF) calcd. For $C_{19}H_{13}F_6N_4S$ $[M+H]^+$ (m/z): 443.0765, found: 443.0665.

3. Characterization spectra

5-Nitro-2,2’-bipyridine:

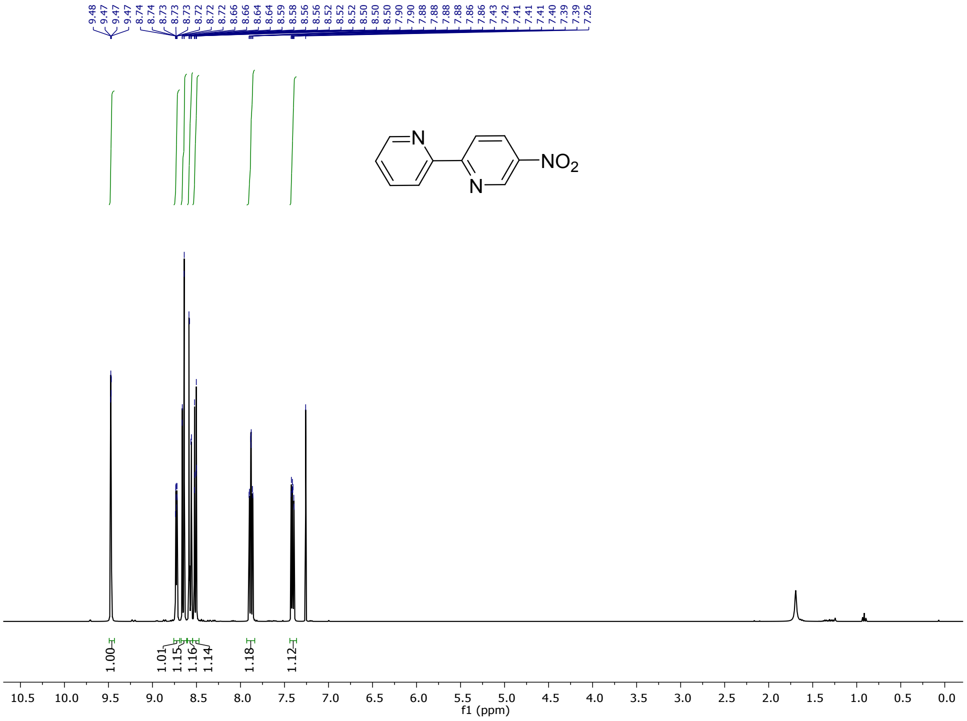

Figure S1. ^{1}H NMR (400 MHz, 298 K in $CDCl_3$) spectrum of 5-Nitro-2,2’-bipyridine.

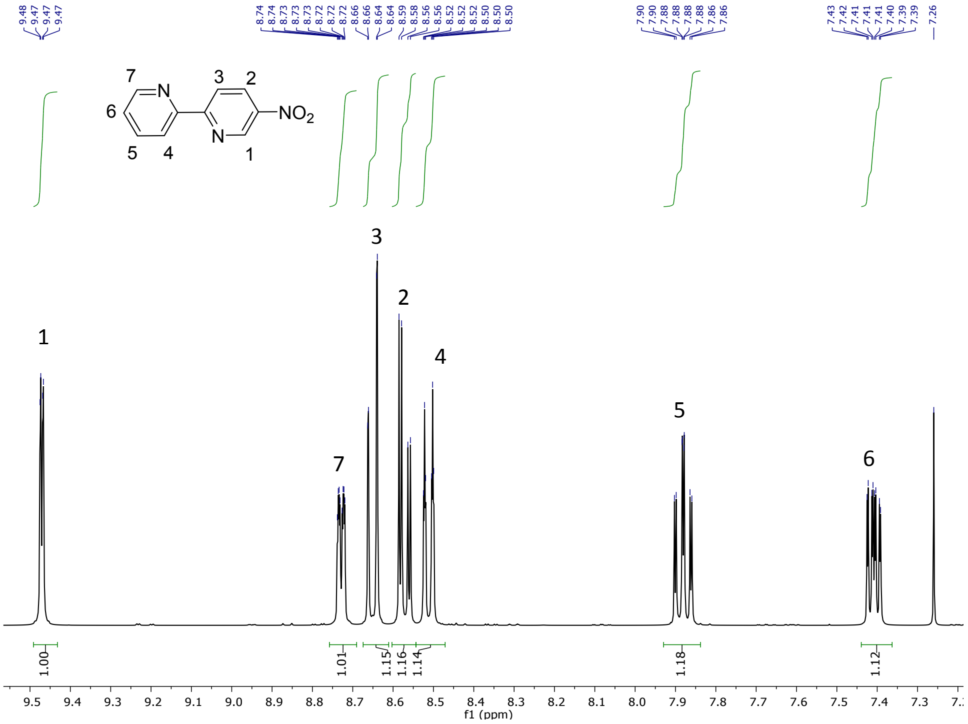

Figure S2. ^{1}H NMR expansion of the aromatic region of 5-Nitro-2,2’-bipyridine.

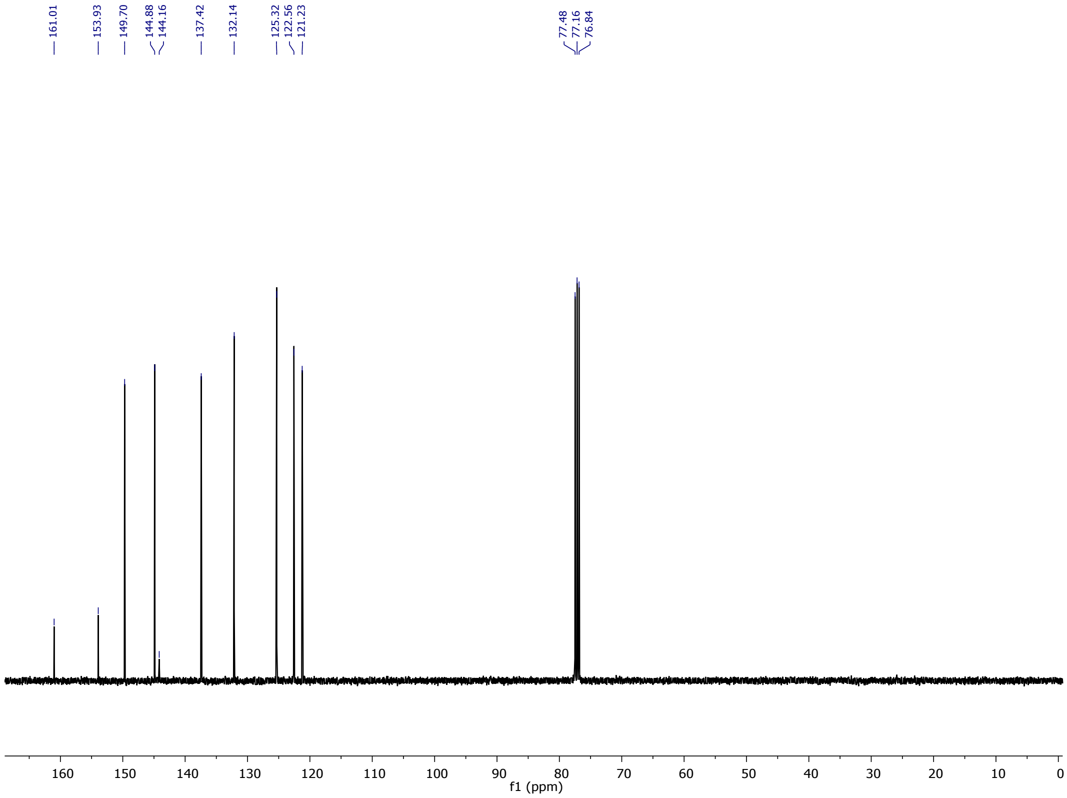

Figure S3. ^{13}C NMR (101 MHz, 298 K in $CDCl_3$) spectrum of 5-Nitro-2,2′-bipyridine.

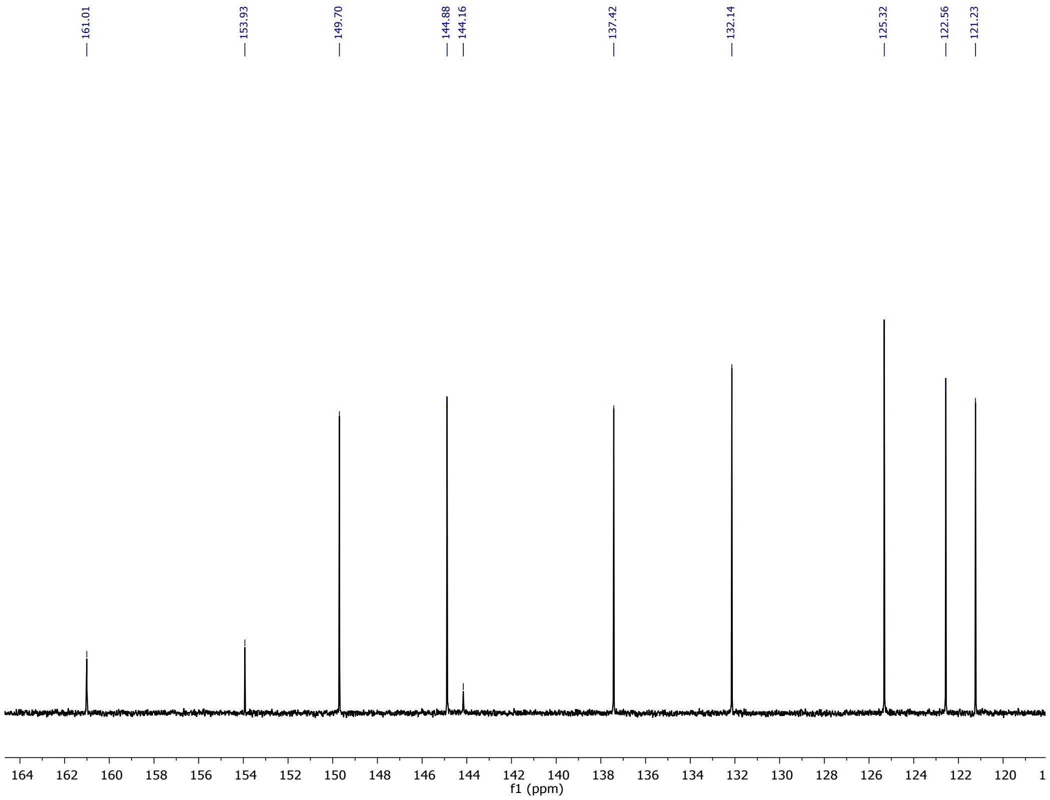

Figure S4. ^{13}C NMR expansion of the aromatic region of 5-Nitro-2,2′-bipyridine.

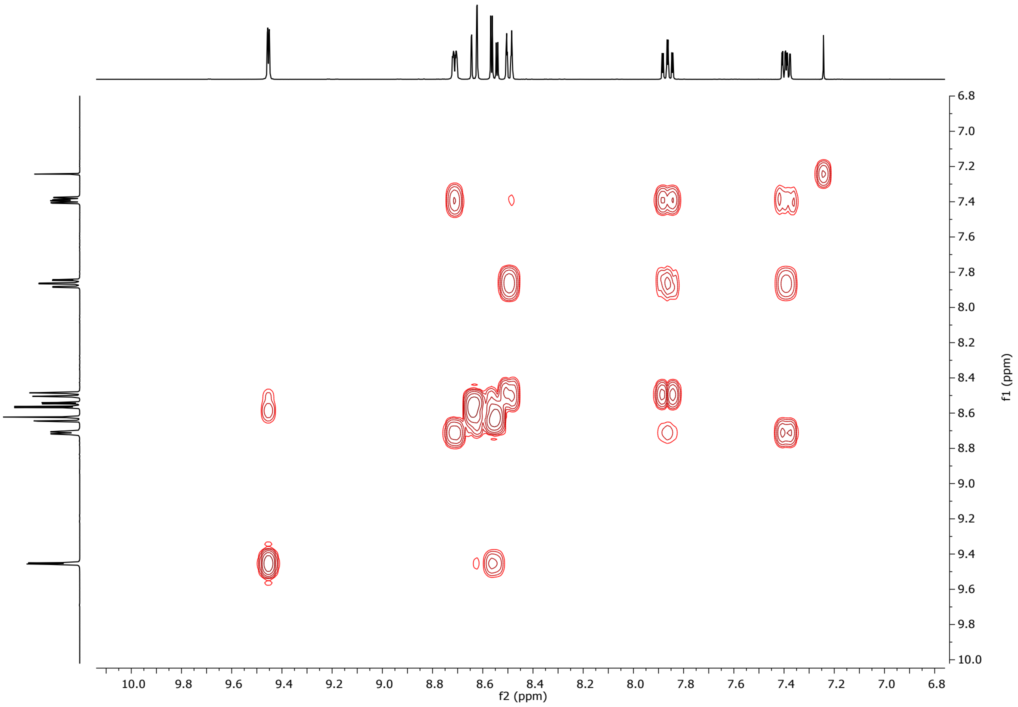

Figure S5. ^{1}H-^{1}H gCOSY (400 MHz, 298 K in CDCl$_3$) spectrum of 5-Nitro-2,2’-bipyridine.

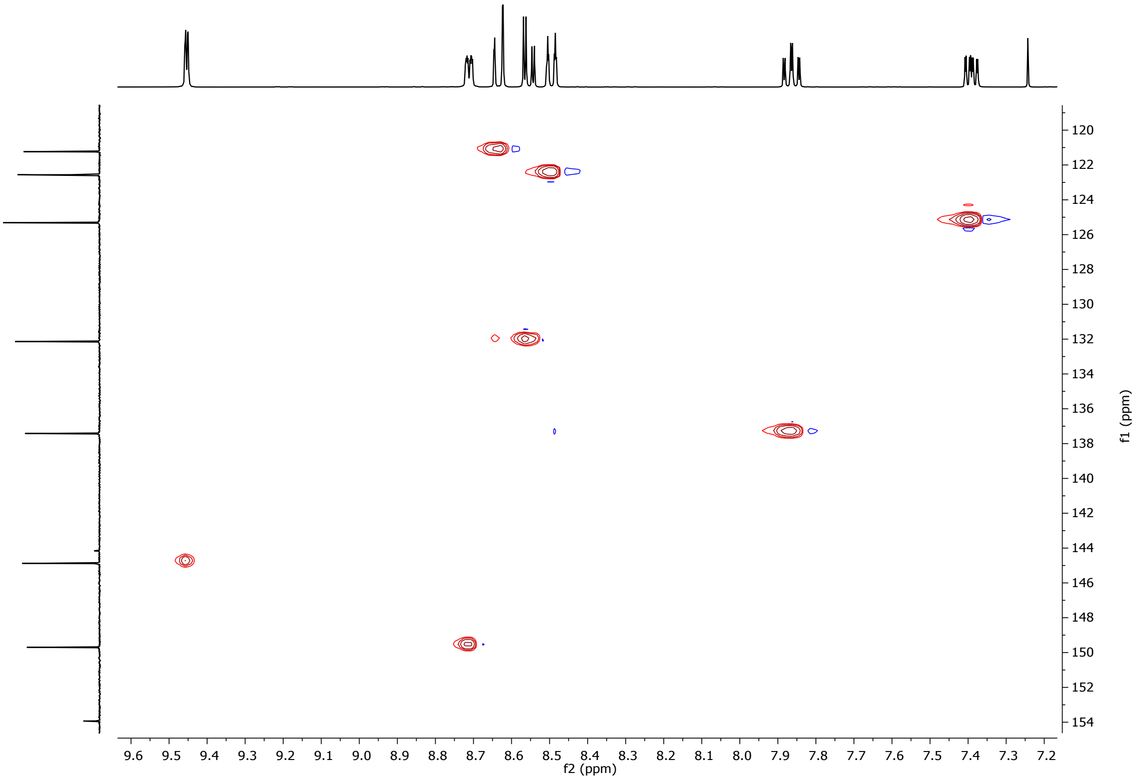

Figure S6. ^{1}H-^{13}C gHSQC (400 MHz, 298 K in CDCl$_3$) spectrum of 5-Nitro-2,2’-bipyridine.

5-Amino-2,2’-bipyridine:

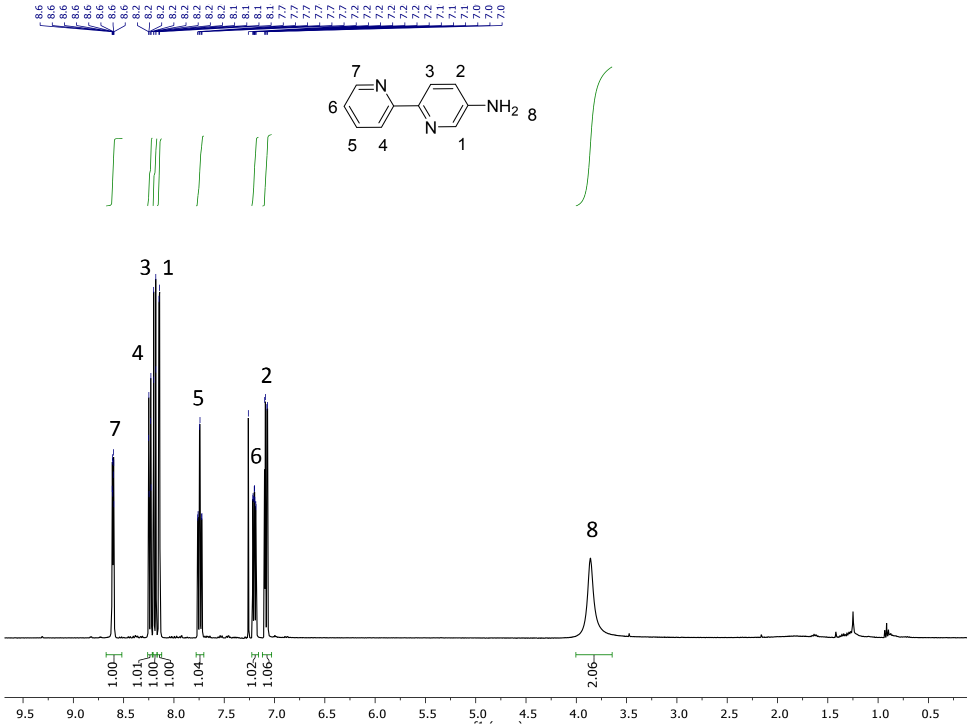

Figure S7. ^{1}H NMR (400 MHz, 298 K in $CDCl_3$) spectrum of 5-Amino-2,2'-bipyridine.

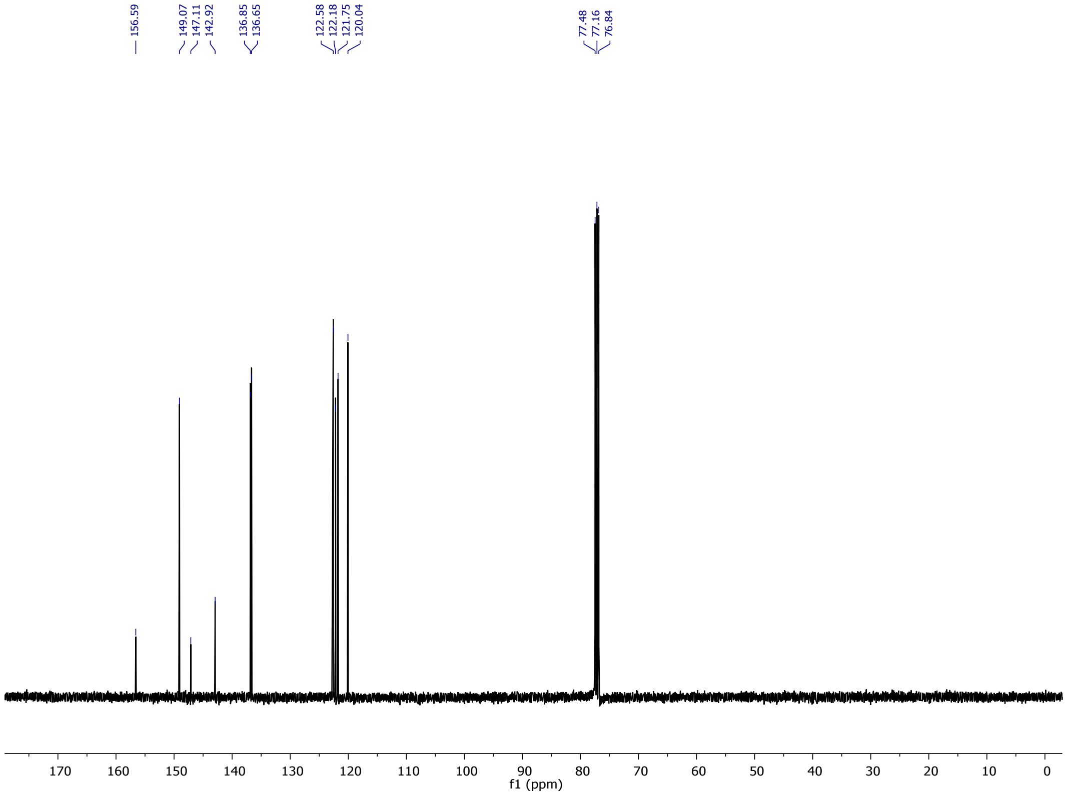

Figure S8. ^{13}C NMR (101 MHz, 298 K in $CDCl_3$) spectrum of 5-Amino-2,2'-bipyridine.

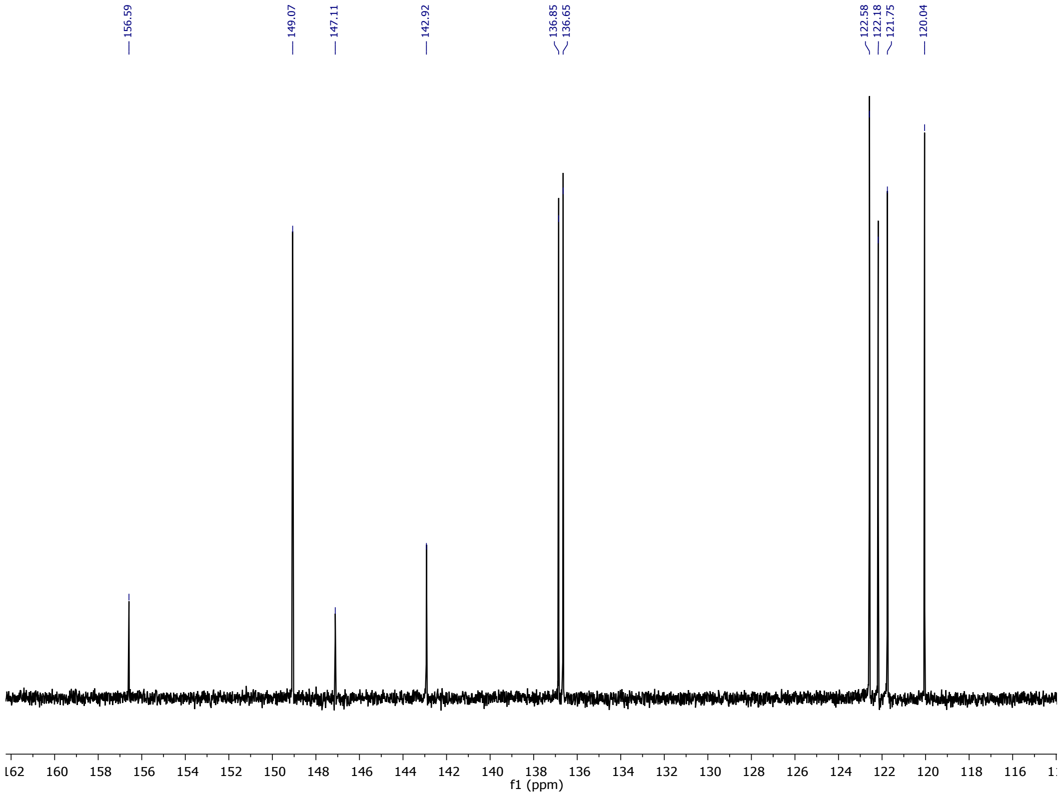

Figure S9. ^{13}C NMR expansion of aromatic region of 5-Amino-2,2’-bipyridine.

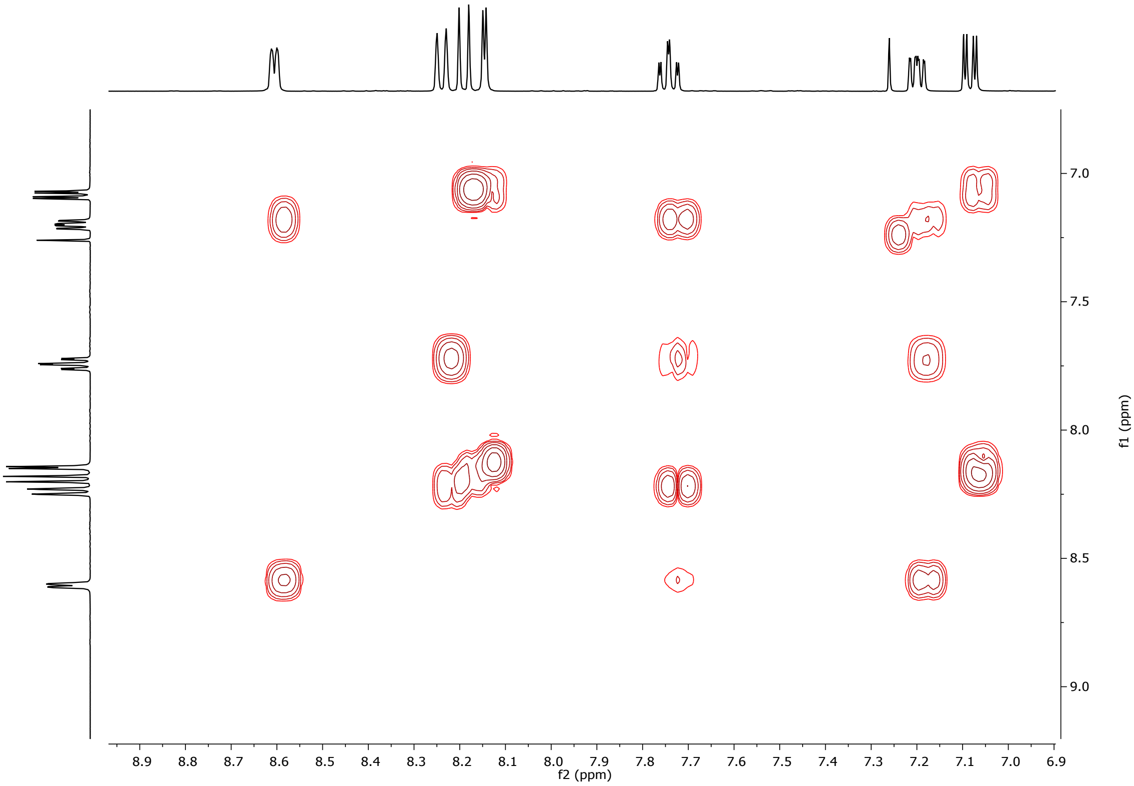

Figure S10. ^{1}H-^{1}H gCOSY (400 MHz, 298 K in $CDCl_3$) spectrum of 5-Amino-2,2’-bipyridine.

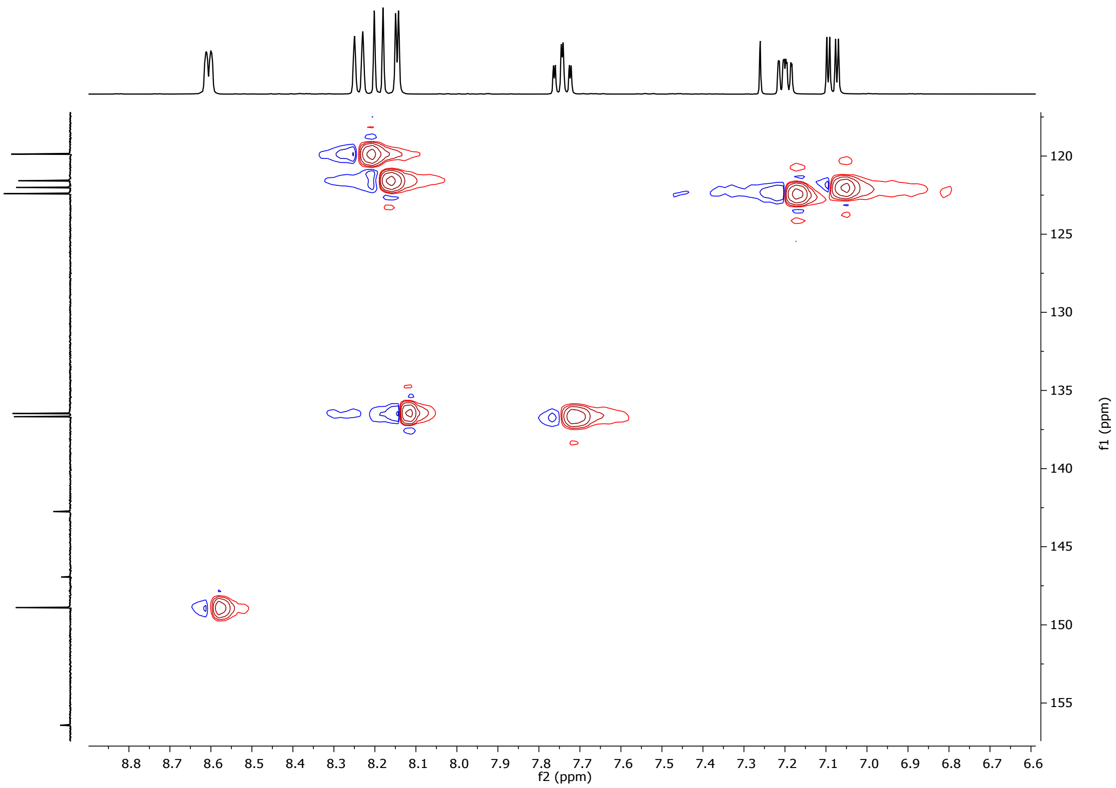

Figure S11. ^{1}H-^{13}C gHSQC (400 MHz, 298 K in $CDCl_3$) spectrum of 5-Amino-2,2’-bipyridine.

Tert-butyl (_S_)-2-([2,2’-bipyridin]-5-ylcarbamoyl)pyrrolidine-1-carboxylate (bipyPro-Boc):

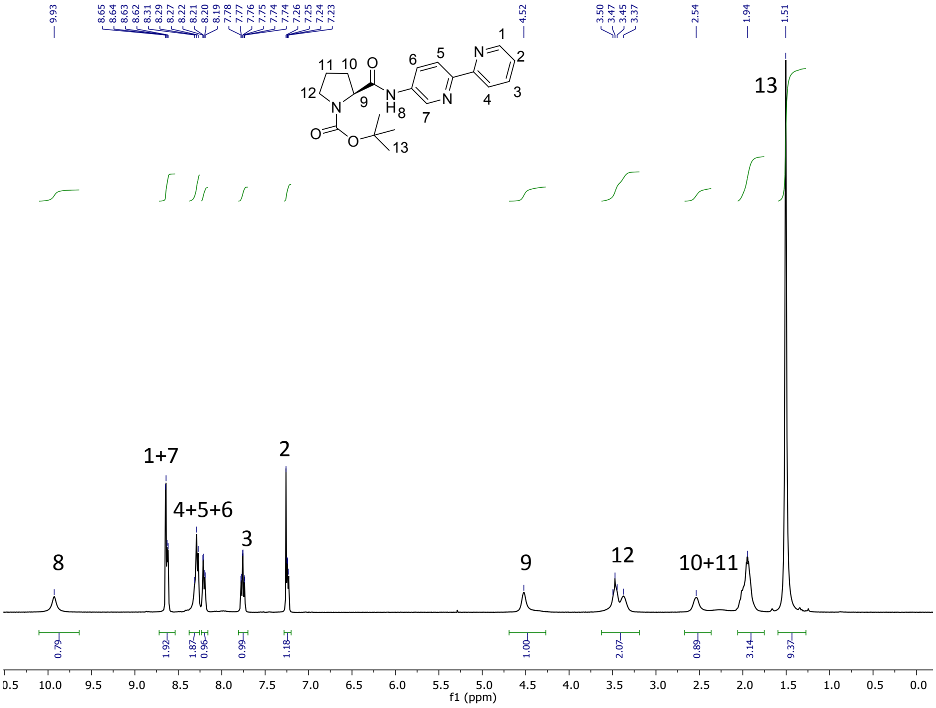

Figure S12. ^{1}H NMR (400 MHz, 298 K in $CDCl_3$) spectrum of bipyPro-Boc.

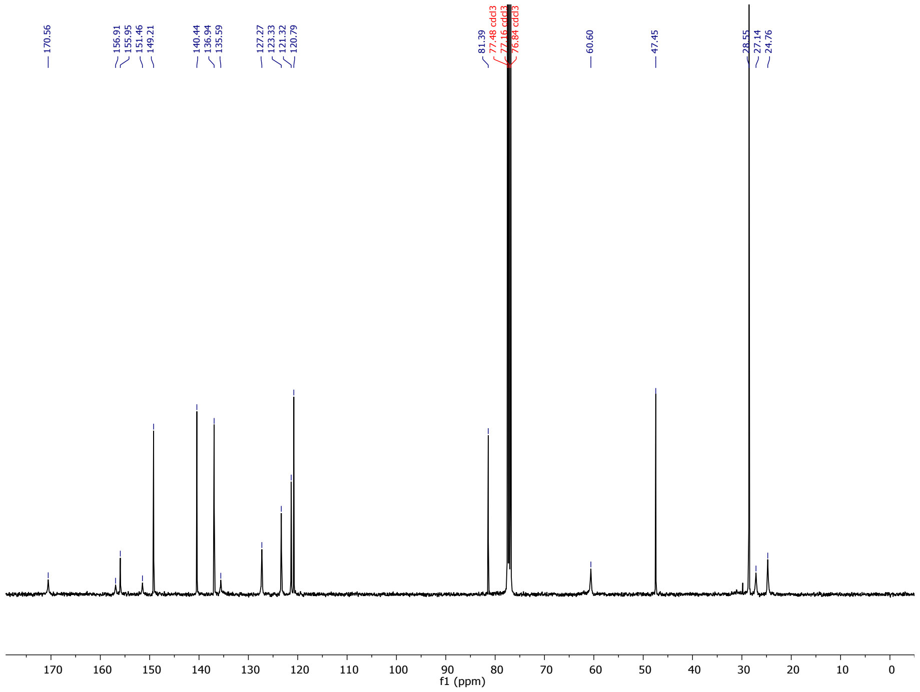

Figure S13. ^{13}C NMR (101 MHz, 298 K in CDCl3) spectrum of bipyPro-Boc.

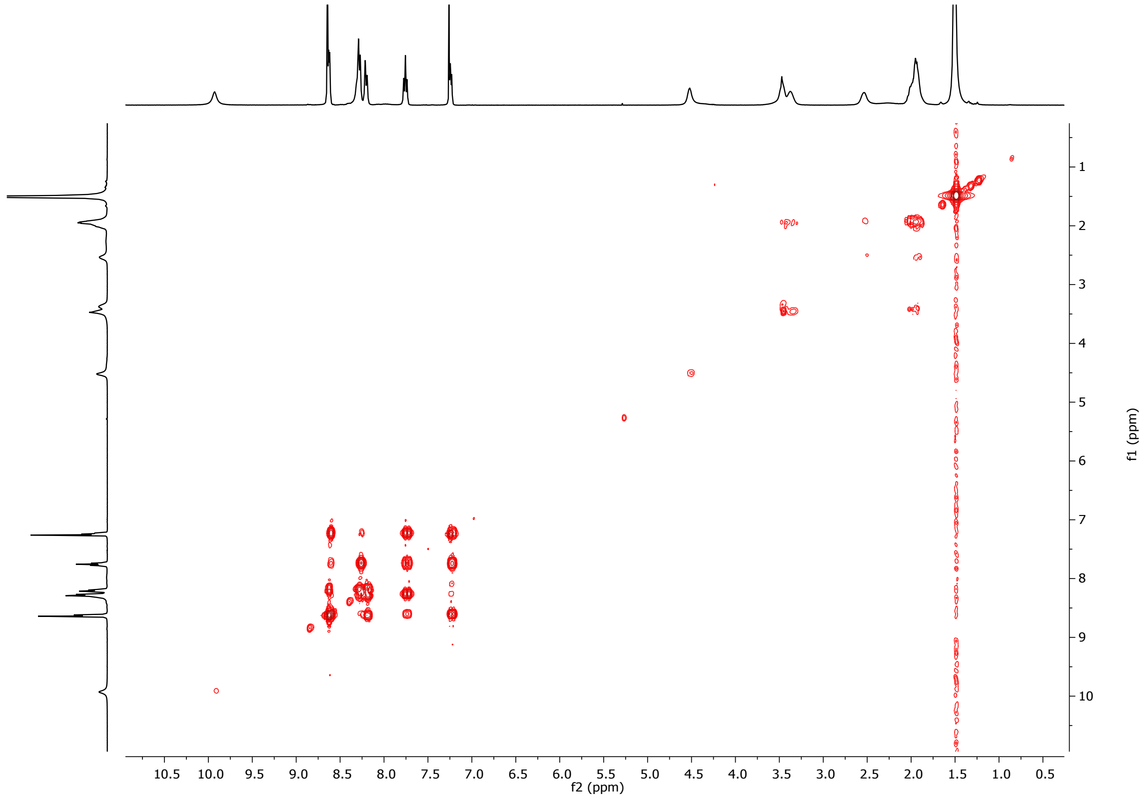

Figure S14. ^{1}H-^{1}H gCOSY (400 MHz, 298 K in CDCl$_3$) spectrum of bipyPro-Boc.

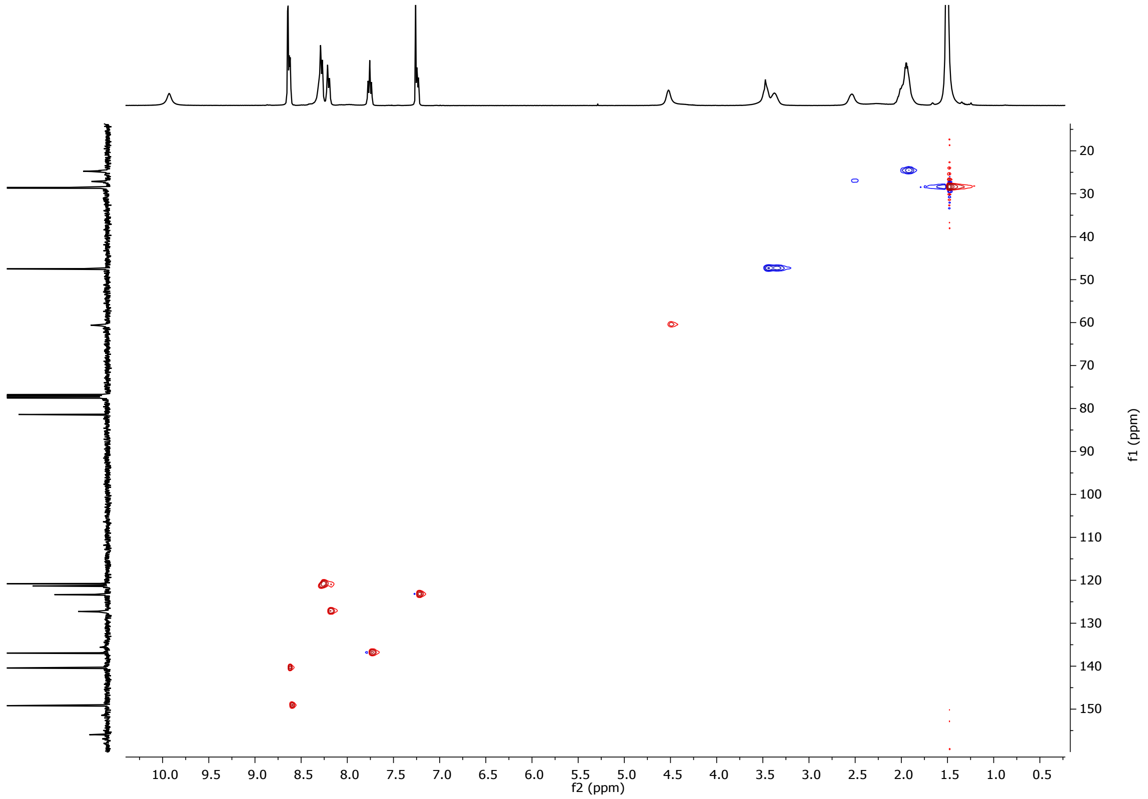

Figure S15. ^{1}H-^{13}C gHSQC (400 MHz, 298 K in CDCl$_3$) spectrum of bipyPro-Boc.

(*S*)-*N*-([2,2’-bipyridin]-5-yl)pyrrolidine-2-carboxamide (bipyPro):

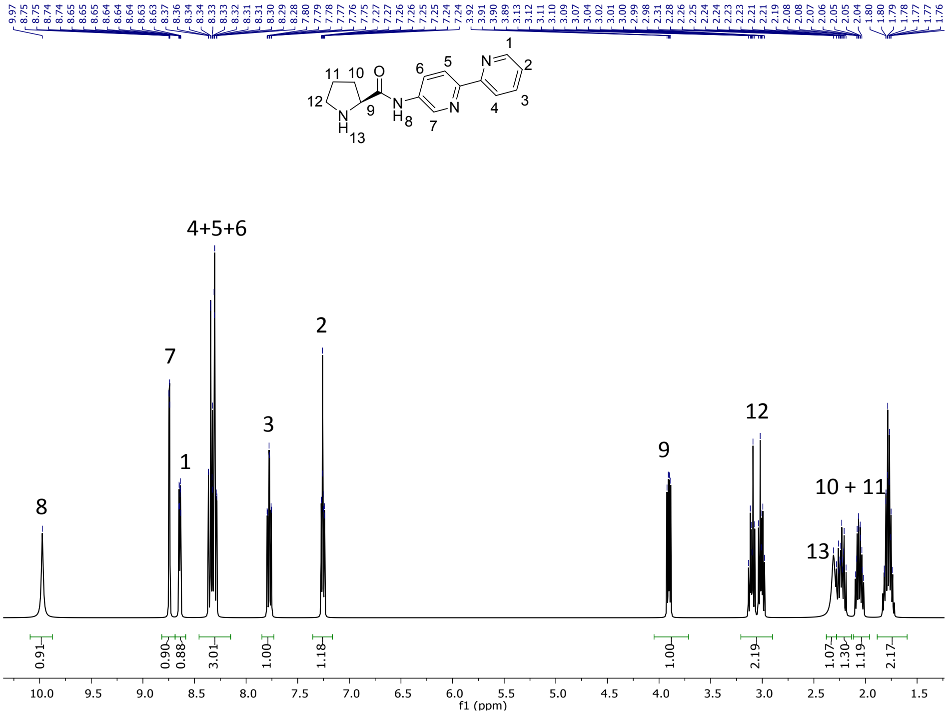

Figure S16. ^{1}H NMR (400 MHz, 298 K in CDCl$_3$) spectrum of bipyPro.

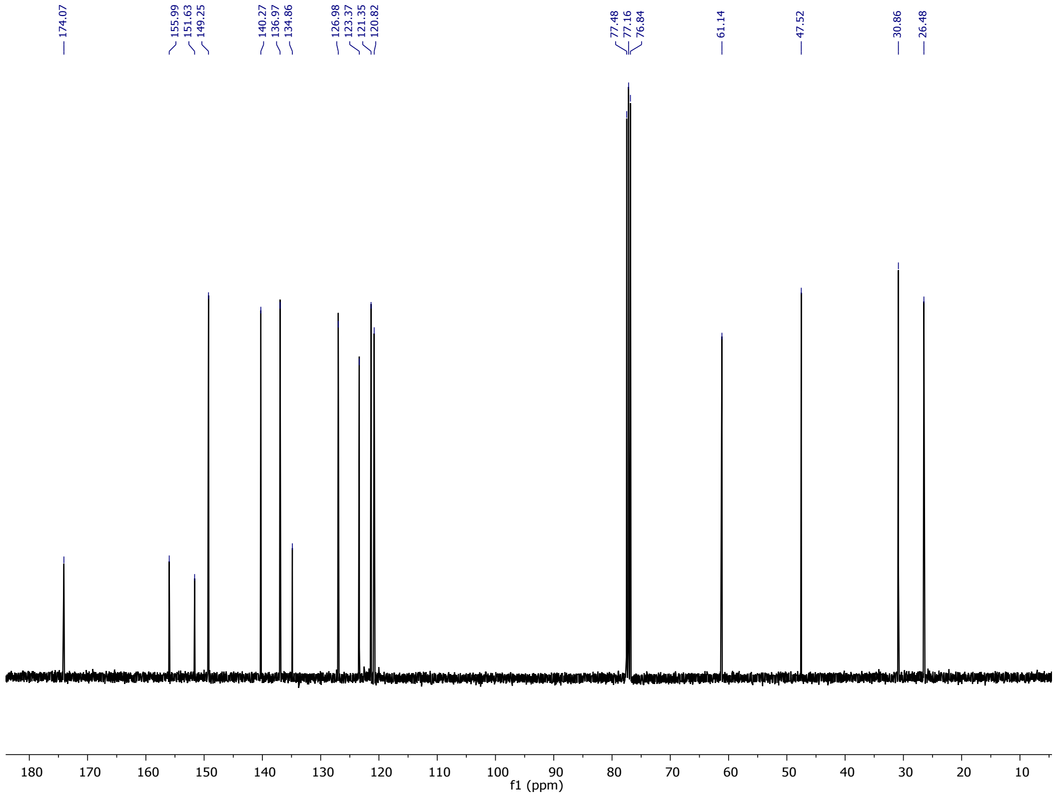

Figure S17. ^{13}C NMR (101 MHz, 298 K in CDCl3) spectrum of bipyPro.

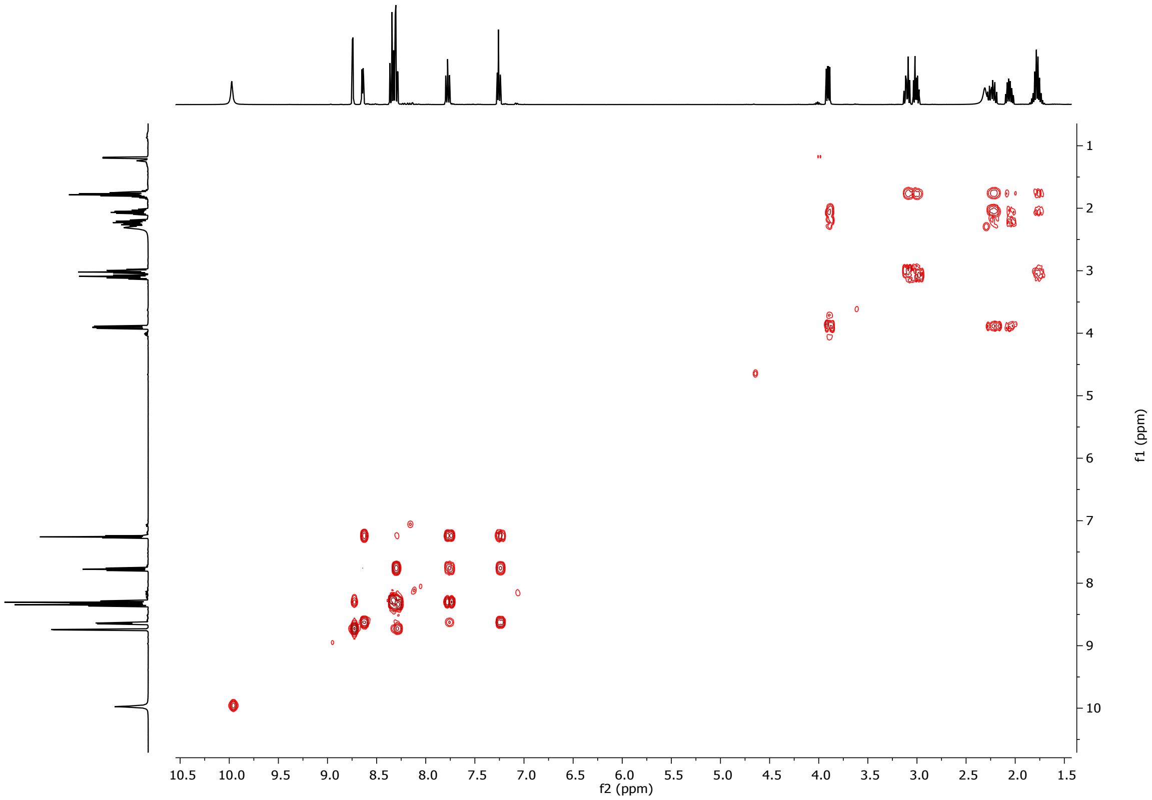

Figure S18. ^{1}H-^{1}H gCOSY (400 MHz, 298 K in CDCl$_3$) spectrum of bipyPro.

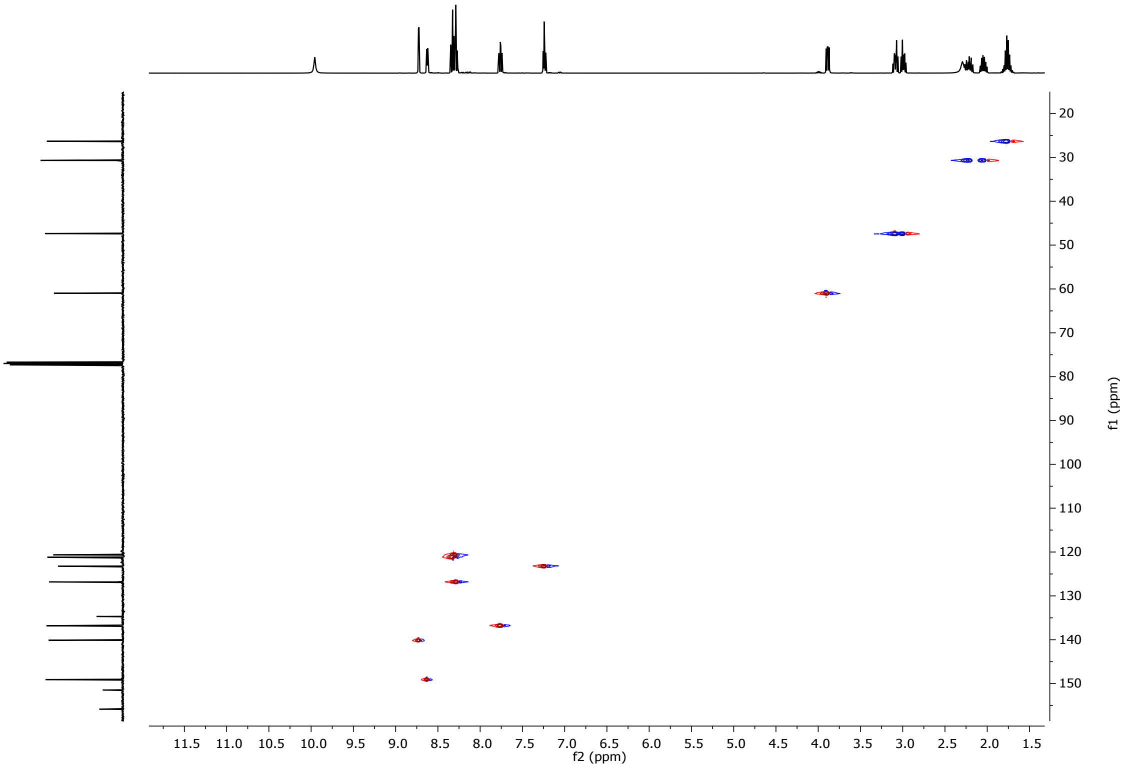

Figure S19. ^{1}H-^{13}C gHSQC (400 MHz, 298 K in $CDCl_3$) spectrum of bipyPro.

1-([2,2'-bipyridin]-5-yl)-3-(3,5-bis(trifluoromethyl)phenyl)thiourea (bipyTU):

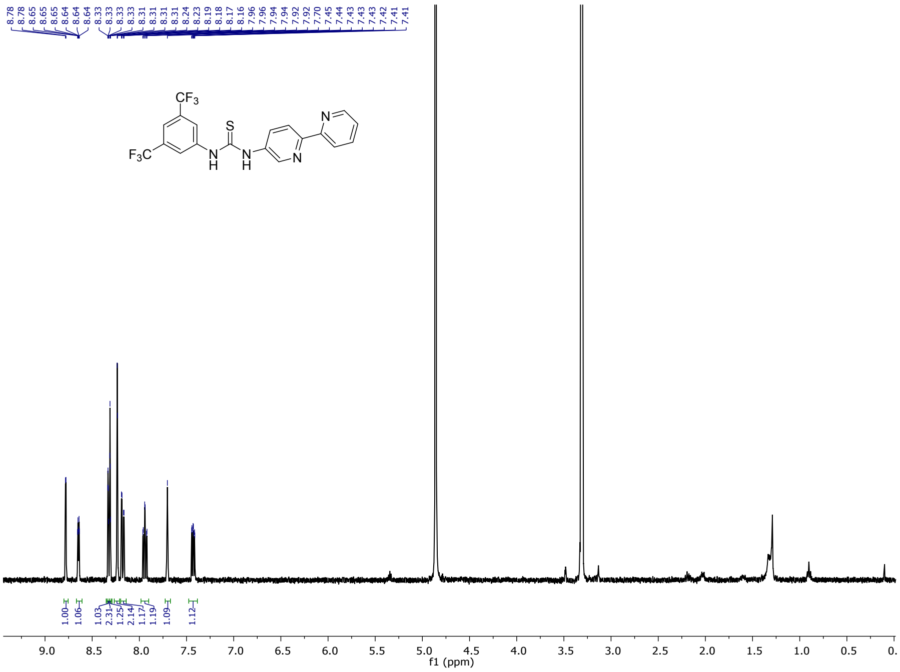

Figure S20. ^{1}H NMR (400 MHz, 298 K in CD_3OD) spectrum of bipyTU.

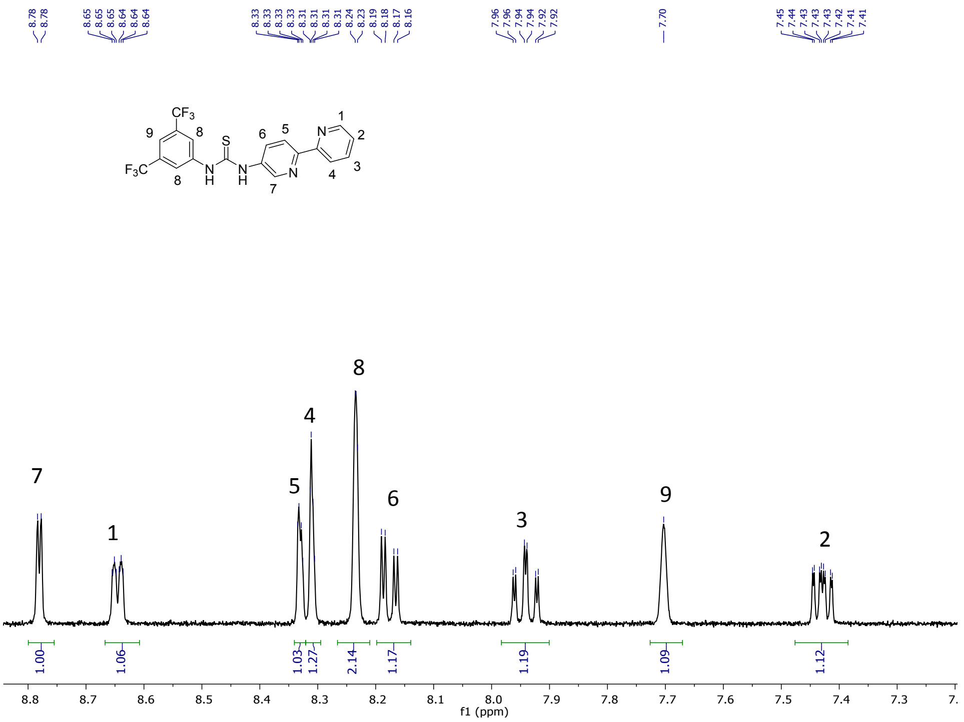

Figure S21. ^{1}H NMR expansion of aromatic region of bipyTU.

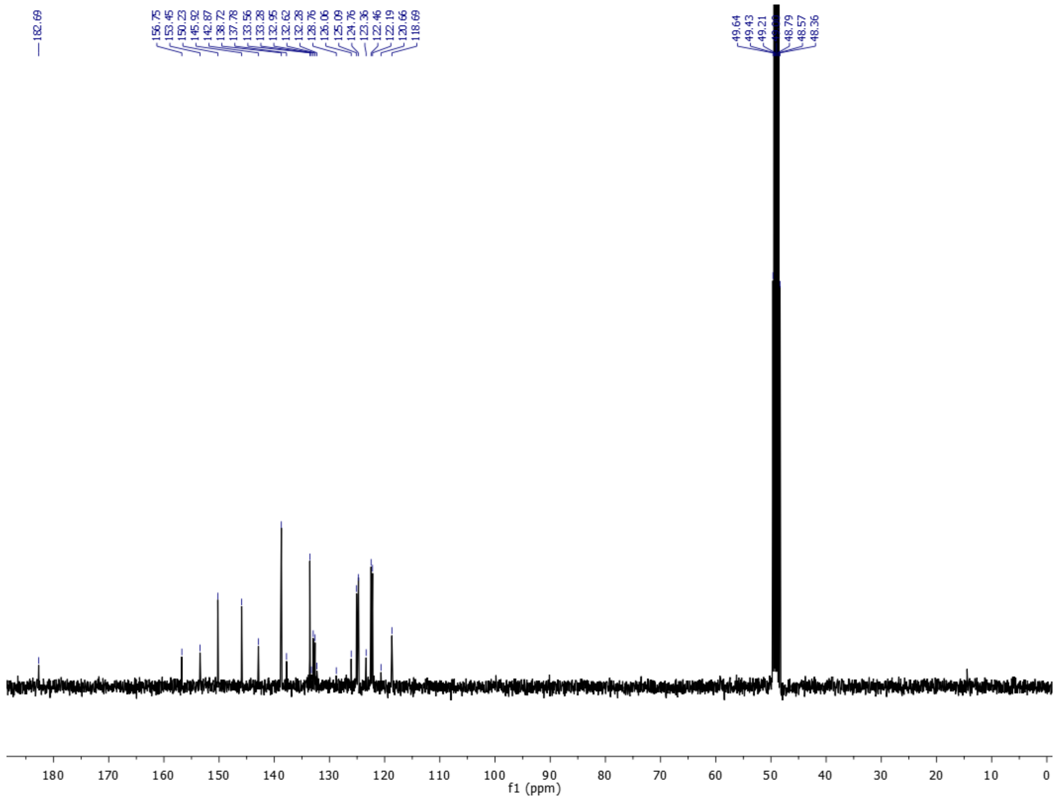

Figure S22. ^{13}C NMR (101 MHz, 298 K in CD_3OD) spectrum of bipyTU.

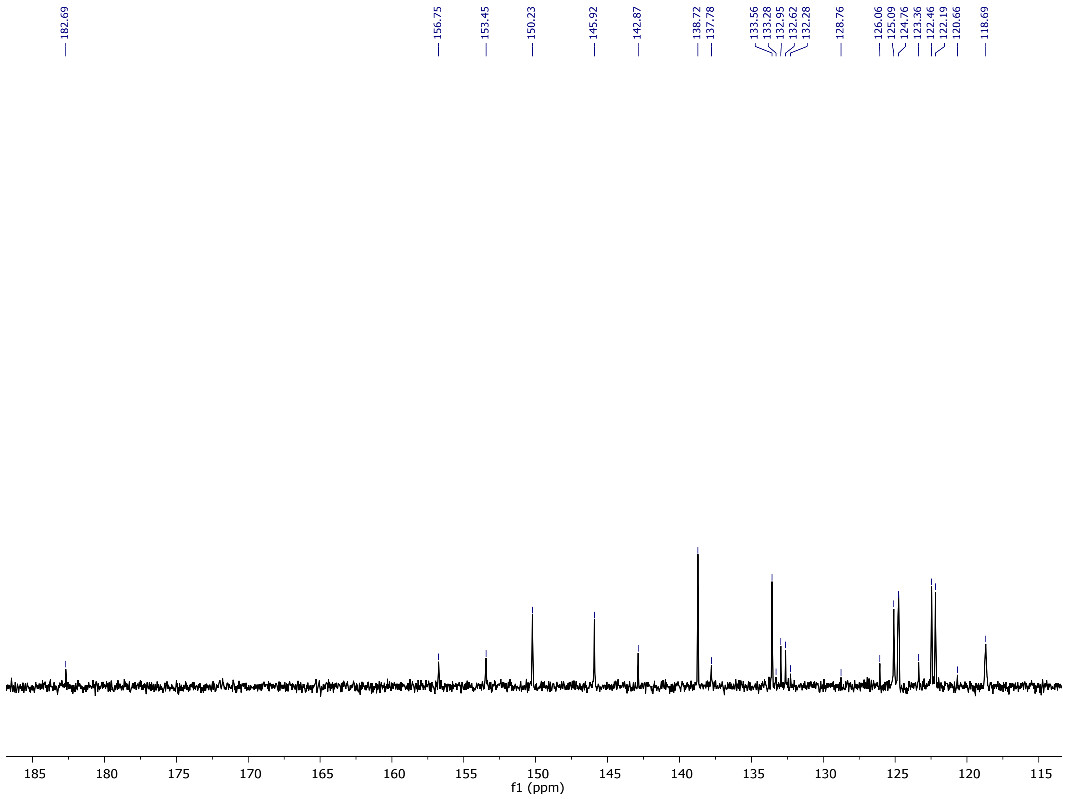

Figure S23. ^{13}C NMR expansion of aromatic region of bipyTU.

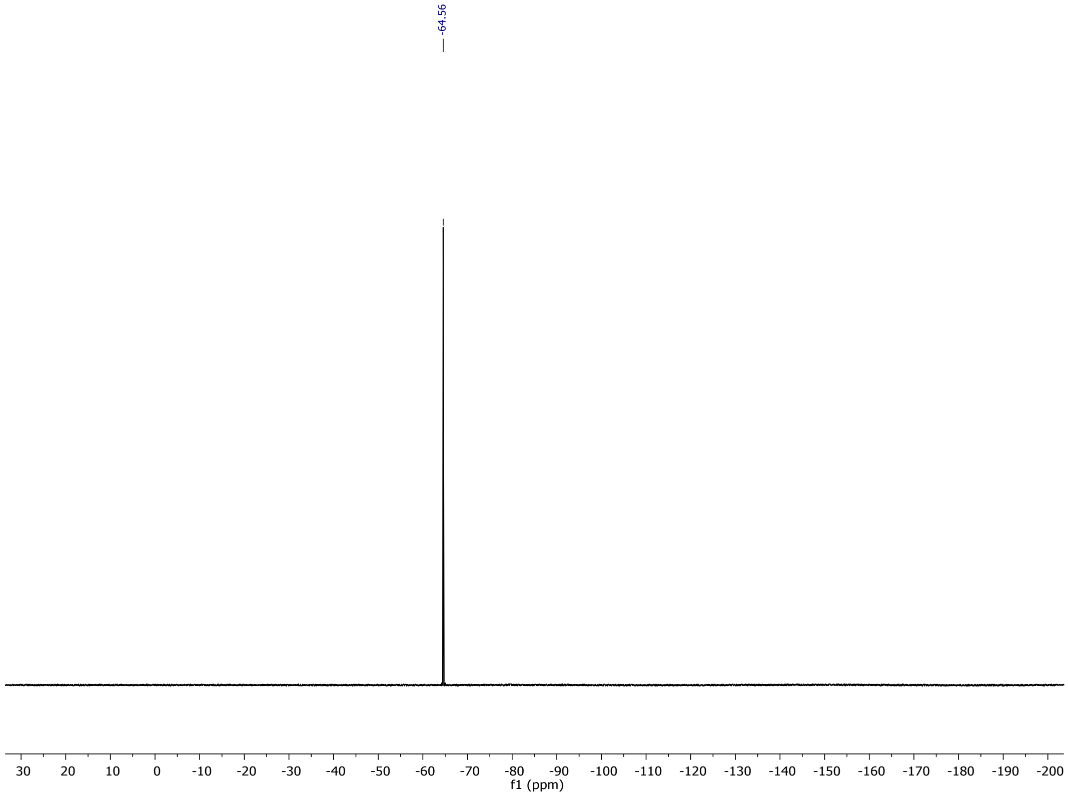

Figure S24. ^{19}F NMR (376 MHz, CD$_3$OD) spectrum of bipyTU.

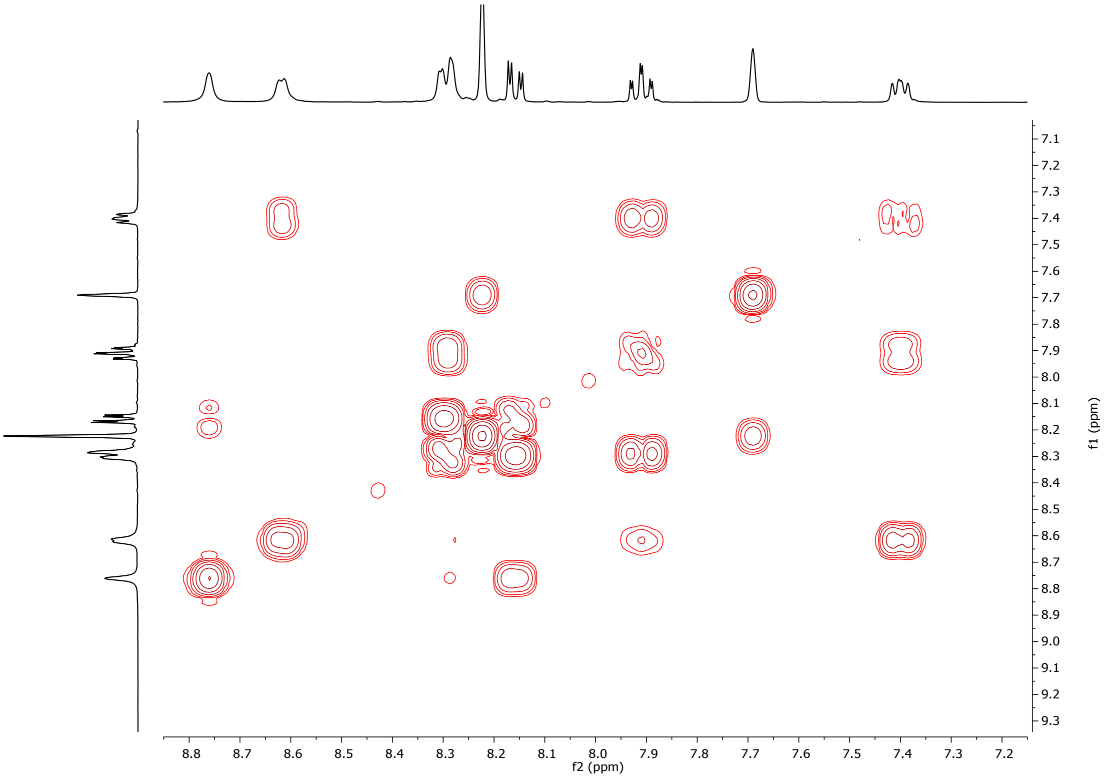

Figure S25. ^{1}H-^{1}H gCOSY (400 MHz, 298 K in CD_3OD) spectrum of bipyTU.

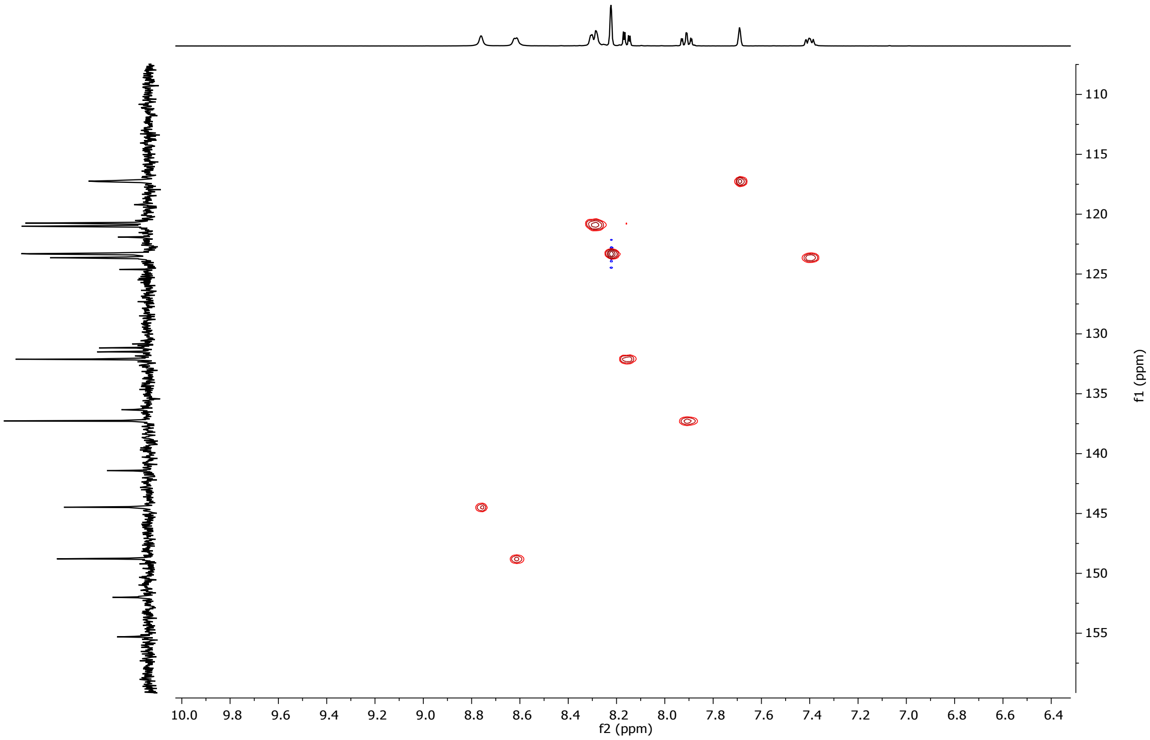

Figure S26. ^{1}H-^{13}C gHSQC (400 MHz, 298 K in CD_3OD) spectrum of bipyTU.

4. General procedure for the asymmetric aldol reaction

A mixture of $Zn(O_2CCF_3)_2.xH_2O$ (5.5 mg, 0.019 mmol, 10 mol %), bipyPro (5 mg, , 0.019 mmol, 10 mol %) and bipyTU (8.4 mg, , 0.019 mmol, 10 mol %,) was stirred in dry THF (300 µL) and H_2O (10 µL, 0.55 mmol, 3 equiv. with respect to aldehyde) at room temperature for 1 h and at 0°C for 30 min. Then, the aldehyde (0.19 mmol) and ketone (1.9 mmol) were added. The resulting mixture was stirred at 0°C for 8-20 h. The reaction was quenched with water and the organic phase was extracted with ethyl acetate (x3). The combined organic layers were dried over anhydrous $MgSO_4$, the solvent was evaporated and the crude product was purified by flash chromatography eluting with hexane/ethyl acetate mixtures of increasing polarity.

^1H NMR on the crude samples was performed to determine conversion and diastereoselectivity. The enantiomeric excess was determined by HPLC on chiral stationary phase (See below for details).

(*S*)-2-((*R*)-hydroxy(phenyl)methyl)cyclohexan-1-one[2-4]:

Chiral analysis was performed using a Chiralpak ID column eluting with n-hexane / isopropanol (97/3) mobile phase, flow 1 mL/min. (Crude product, *ca*. 40% conversion): 96% ee

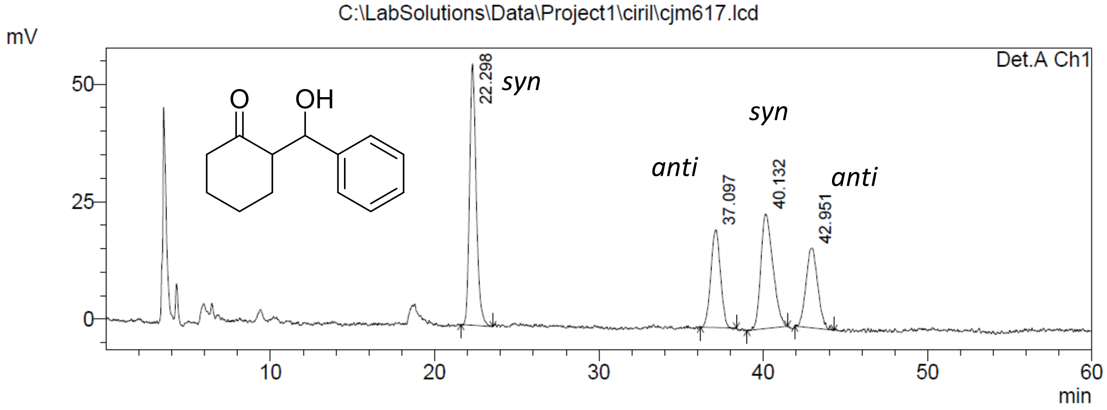

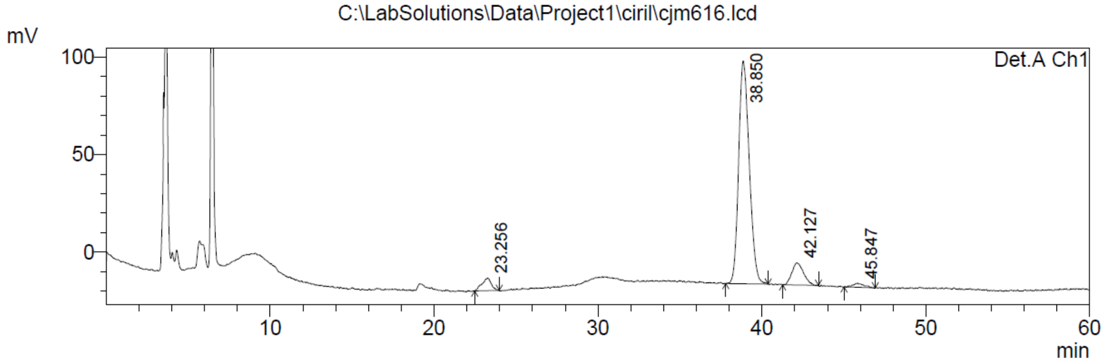

(*S*)-2-((*R*)-hydroxy(4-nitrophenyl)methyl)cyclohexan-1-one[2-4]:

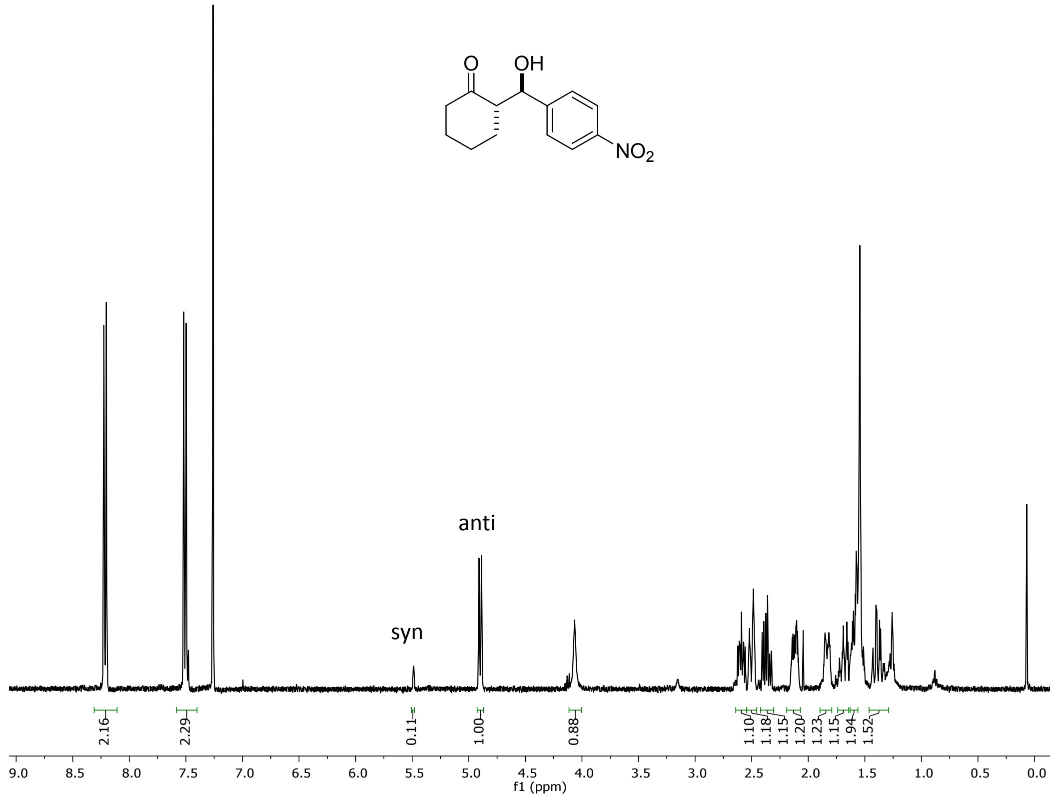

^{1}H NMR (400 MHz, $CDCl_3$) δ (ppm) 8.21 (d, J = 8.8 Hz, 2H), 7.49 (d, J = 8.6 Hz, 2H), 4.90 (d, J = 8.4 Hz, 1H), 4.06 (bs, 1H), 2.59 (m, 1H), 2.53 – 2.45 (m, 1H), 2.37 (m, 1H), 2.12 (m, 1H), 1.83 (m, 1H), 1.67 (m, 1H), 1.63 – 1.56 (m, 2H), 1.38 (m, 1H). **$[\alpha]^{20}_D$=** + 9.1 (c = 0.96, $CHCl_3$). Lit.: +11.0 (c = 0.26, $CHCl_3$, 94% ee).

Chiral analysis was performed using a Chiralcel OD-H column eluting with n-hexane/ isopropanol (97/3) mobile phase, flow 1 mL/min.

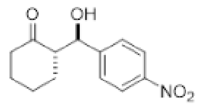

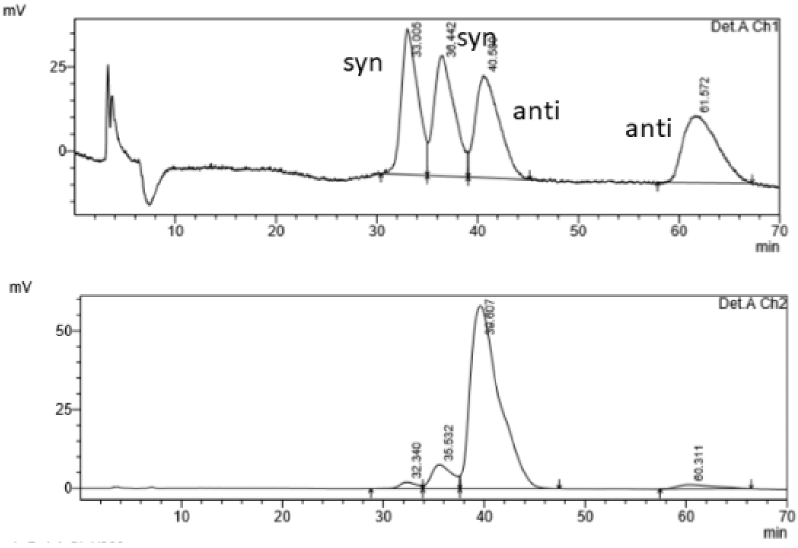

(*S*)-2-((*R*)-(2-chlorophenyl)(hydroxy)methyl)cyclohexan-1-one[2-4]:

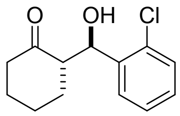

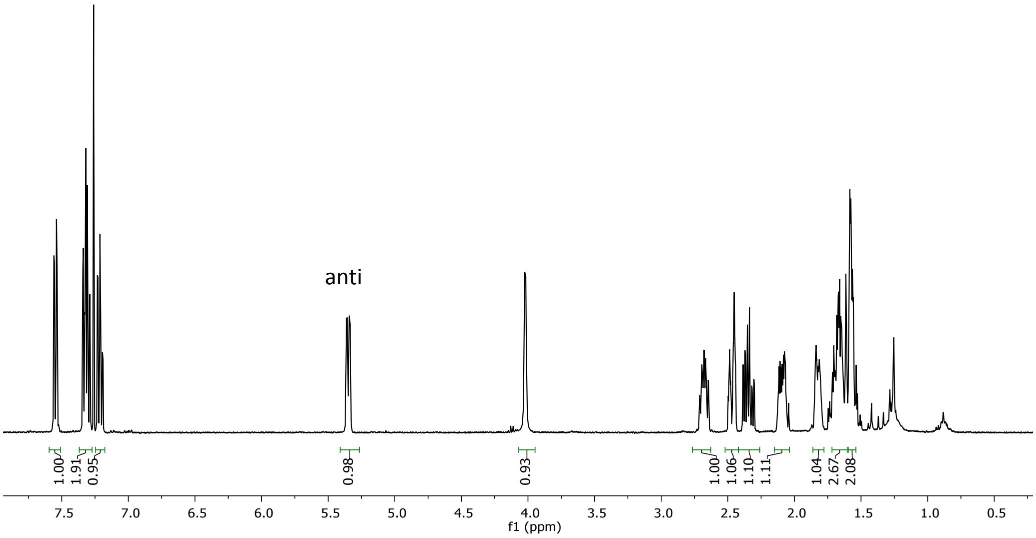

^{1}H NMR (400 MHz, $CDCl_3$) δ (ppm) 7.52 (m, 1H), 7.34 – 7.25 (m, 2H), 7.22 – 7.14 (m, 1H), 5.33 (dd, *J* = 8.2, 3.8 Hz, 1H), 4.02 (d, J = 3.4 Hz, 1H), 2.68 (m, 1H), 2.47 (m, 1H), 2.37 – 2.26 (m, 1H), 2.06 (m, 1H), 1.79 (m, 1H), 1.74 – 1.60 (m, 2H), 1.59 – 1.48 (m, 2H).

Chiral analysis was performed using a Chiralpak ID column eluting with n-hexane/isopropanol (97/3) mobile phase, flow 1 mL/min.

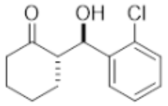

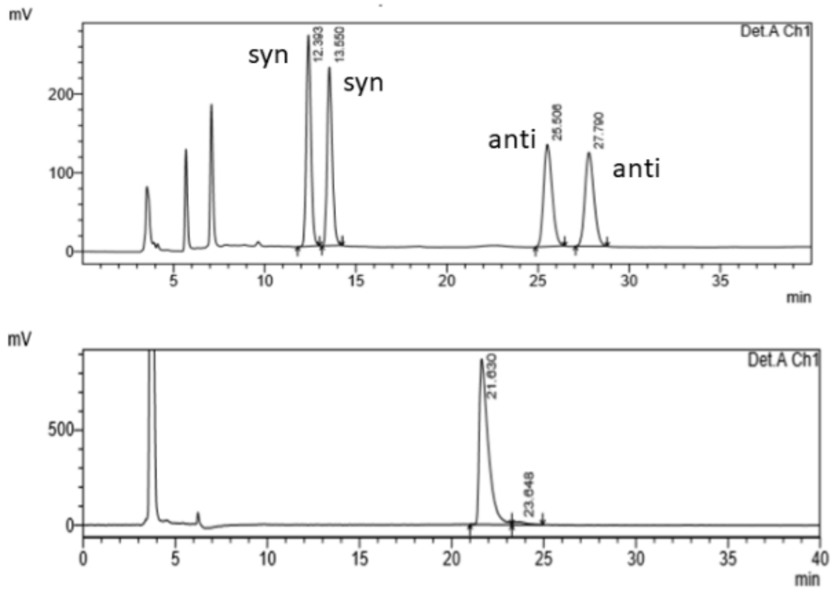

(*S*)-2-((*R*)-(3-fluorophenyl)(hydroxy)methyl)cyclohexan-1-one[2-4]:

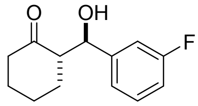

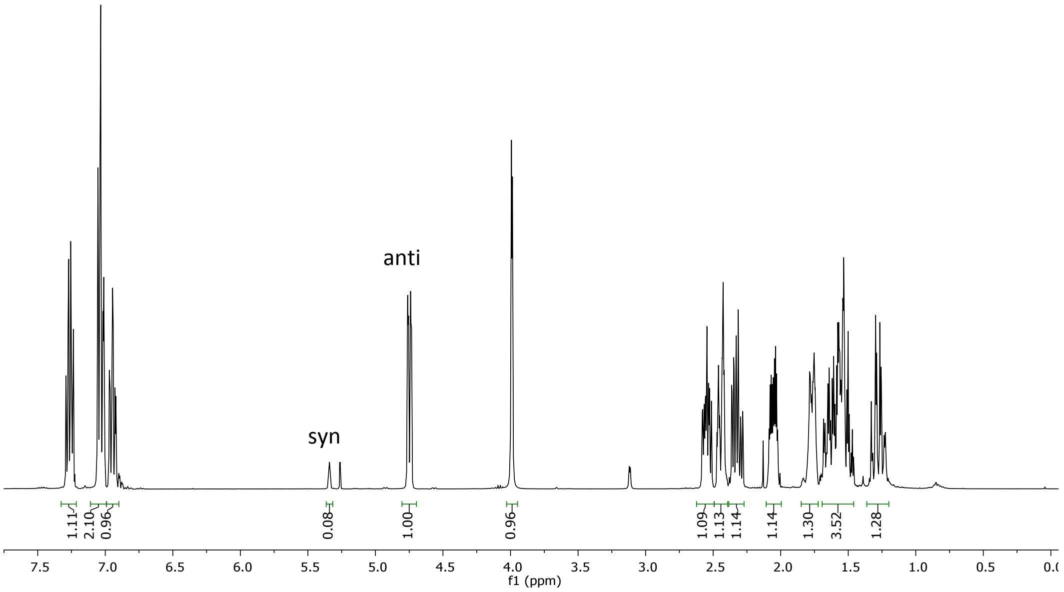

¹H NMR (400 MHz, $CDCl_3$) δ (ppm) 7.30 (m, 1H), 7.17 (m, 2H), 7.01 (m, 1H), 4.69 (dd, *J* = 8.7, 2.5 Hz, 1H), 3.99 (d, *J* = 2.8 Hz, 1H), 2.55 (m, 1H), 2.44 (m, 1H), 2.41 – 2.23 (m, 1H), 2.05 (m, 1H), 1.77 (m, 1H), 1.71 – 1.41 (m, 3H), 1.40 (m, 1H).

Chiral analysis was performed using a Chiralpak ID column eluting with n-hexane / isopropanol (97/3) mobile phase, flow 1 mL/min.

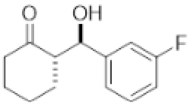

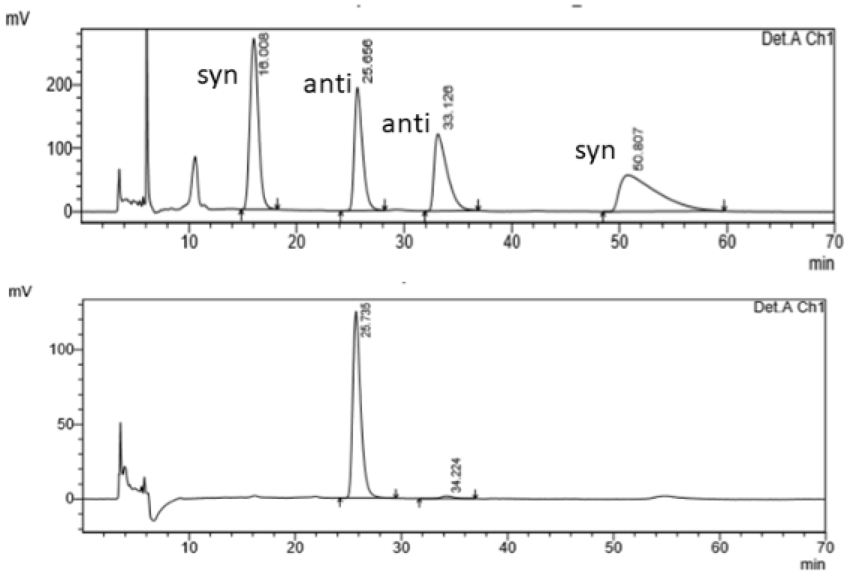

(*S*)-2-((*R*)-hydroxy(4-(trifluoromethyl)phenyl)methyl)cyclohexan-1-one[2-4]:

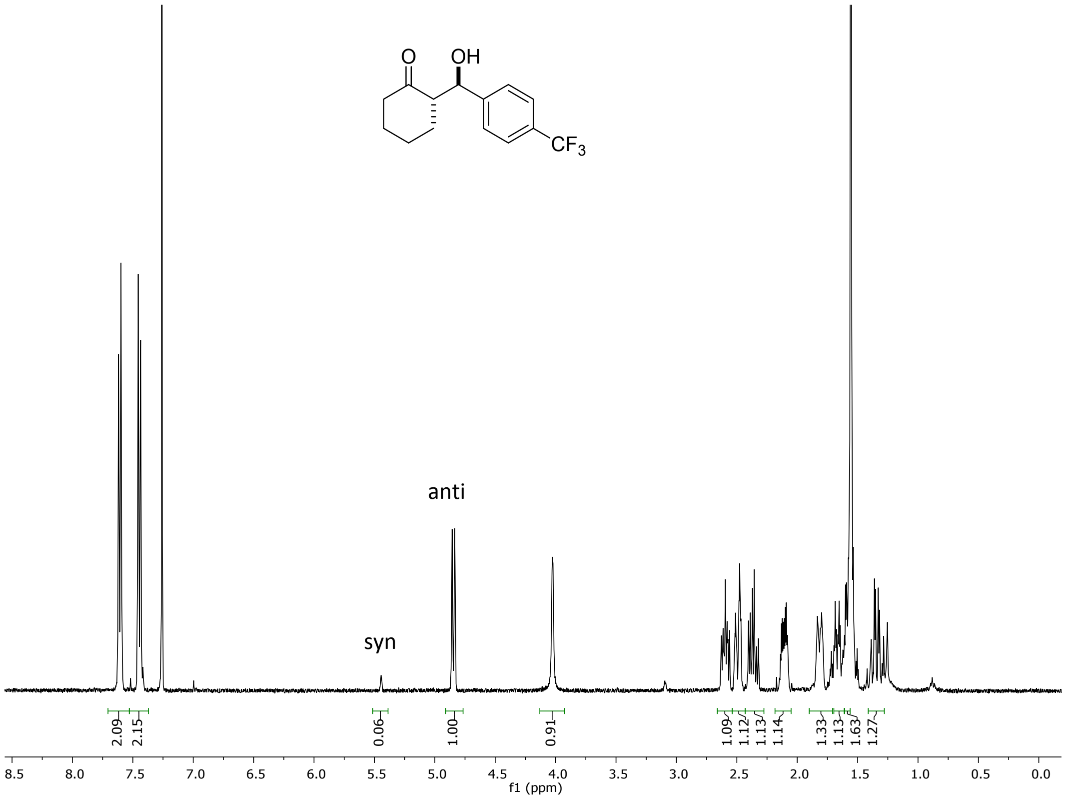

^{1}H NMR (400 MHz, $CDCl_3$) δ (ppm) 7.61 (d, *J* = 8.0 Hz, 2H), 7.45 (d, *J* = 8.0 Hz, 2H), 4.85 (d, *J* = 8.6 Hz, 1H), 4.03 (s, 1H), 2.59 (m, 1H), 2.49 (m 1H), 2.36 (m, 1H), 2.11 (m, 1H), 1.81 (m, 1H), 1.66 (m, 1H), 1.60 – 1.44 (m, 2H), 1.41 – 1.28 (m, 1H).

Chiral analysis was performed using a Chiralpak ID column eluting with n-hexane / isopropanol (97/3) mobile phase, flow 1 mL/min.

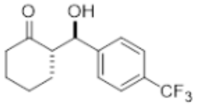

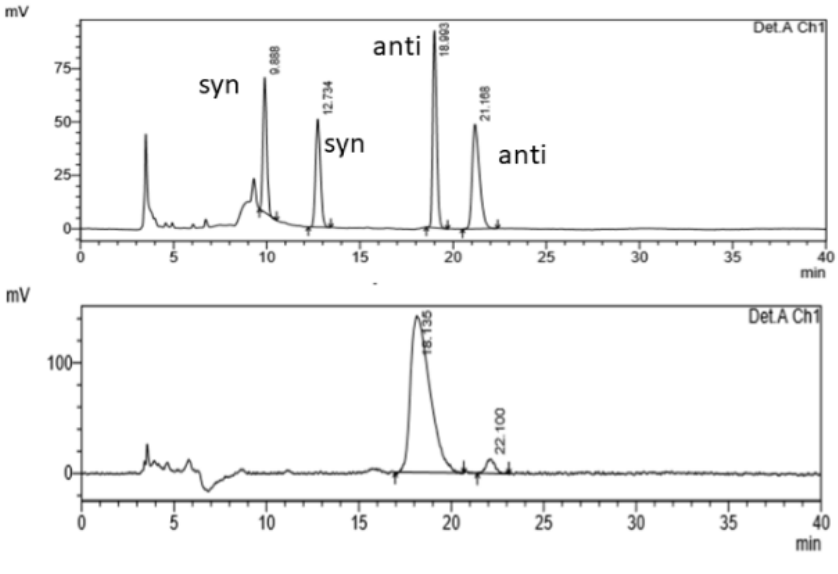

(*S*)-7-((*R*)-hydroxy(4-nitrophenyl)methyl)-1,4-dioxaspiro[4.5]decan-8-one[5]:

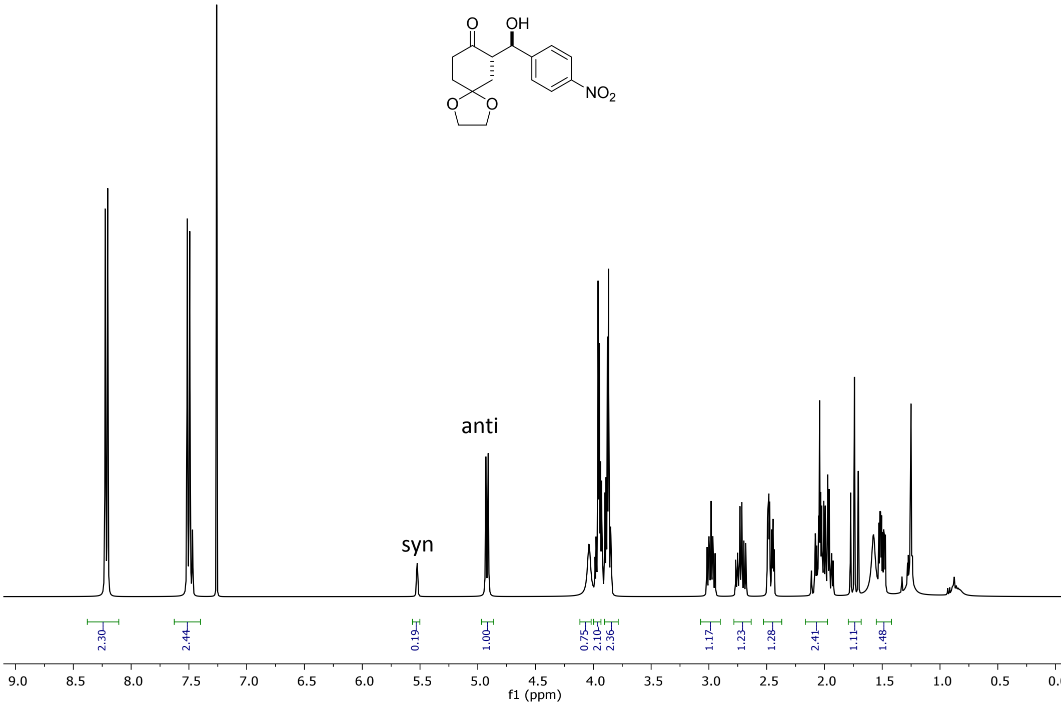

^{1}H NMR (400 MHz, $CDCl_3$) δ (ppm) 8.25 (m, 2H), 7.50 (m, 2H), 4.92 (d, *J* = 8.2 Hz, 1H), 4.04 (bs, 1H), 3.98 – 3.92 (m, 2H), 3.90 – 3.84 (m, 2H), 2.98 (m, 1H), 2.72 (m, 1H), 2.56 – 2.40 (m, 1H), 2.13 – 1.92 (m, 2H), 1.74 (t, *J* = 13.3 Hz, 1H), 1.52 (m, 1H).

Chiral analysis was performed using a Chiralpak IB column eluting with n-hexane / isopropanol (97/3) mobile phase, flow 0.8 mL/min.

.

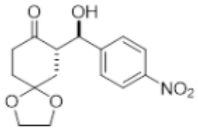

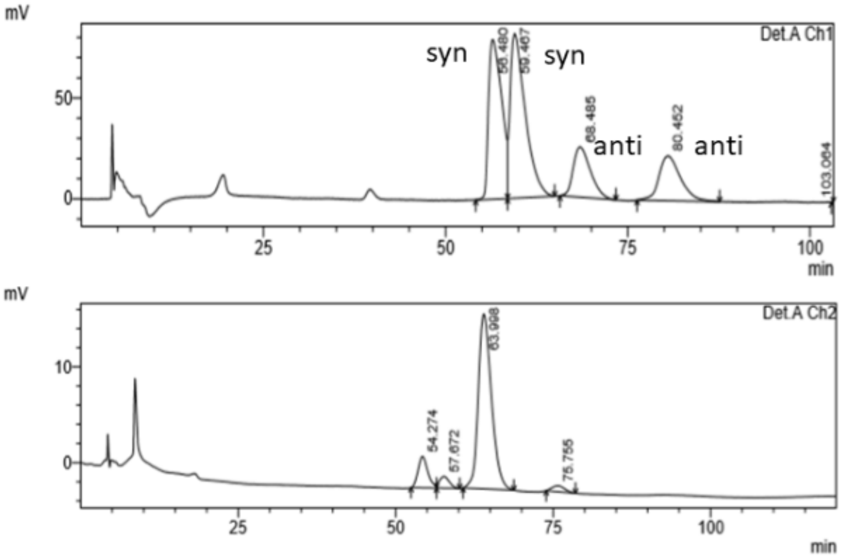

(*R*)-2-((*R*)-hydroxy(4-nitrophenyl)methyl)cyclopentan-1-one/ (*S*)-2-((*R*)-hydroxy(4-nitrophenyl)methyl)cyclopentan-1-one[2-4]:

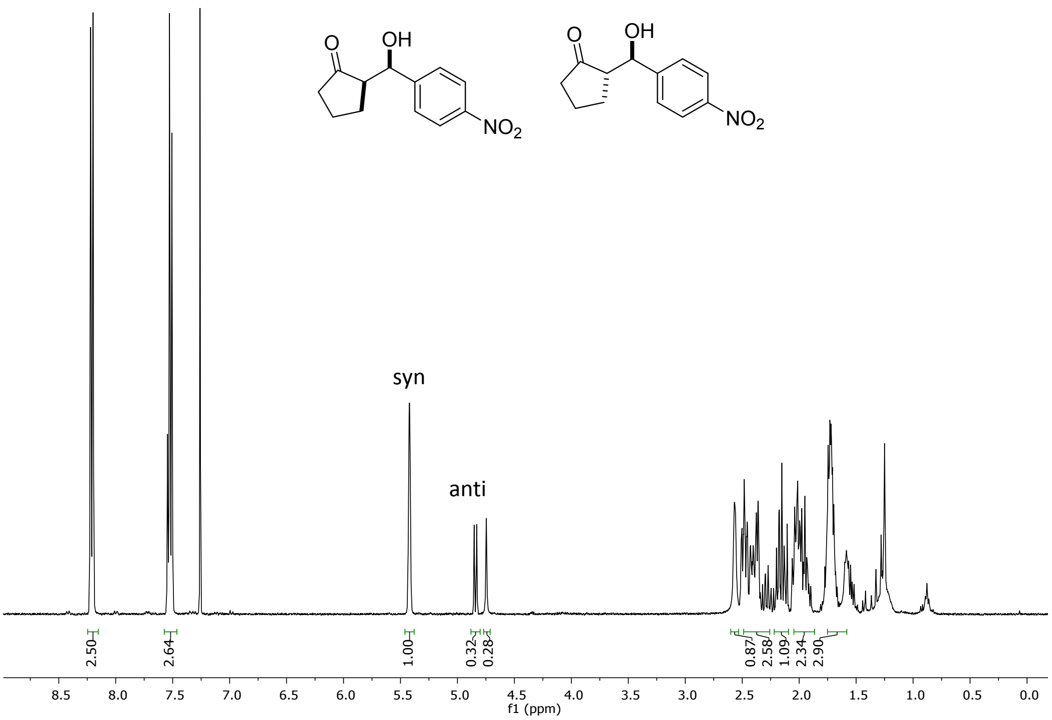

^{1}H NMR (400 MHz, $CDCl_3$, *syn* diastereomer) δ (ppm) 8.19 (m, 2H), 7.48 (m, 2H), 5.40 (m, 1H), 2.58 (m, 1H), 2.51 – 2.31 (m, 2H), 2.19 (m, 1H), 2.07 – 1.87 (m, 2H), 1.80 – 1.63 (m, 2H).

^{1}H NMR (400 MHz, $CDCl_3$, *anti* diastereomer) δ (ppm) 8.19 (m, 2H), 7.48 (m, 2H), 4.82 (m, 1H), 4.72 (s, 1H), 2.51 – 2.31 (m, 2H), 2.19 (m, 1H), 2.07 – 1.87 (m, 2H), 1.80 – 1.63 (m, 2H).

Chiral analysis was performed using a Chiralpak IC column eluting with n-hexane / isopropanol (90/10) mobile phase, flow 1 mL/min.

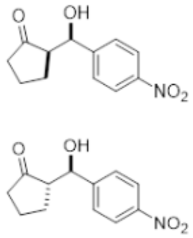

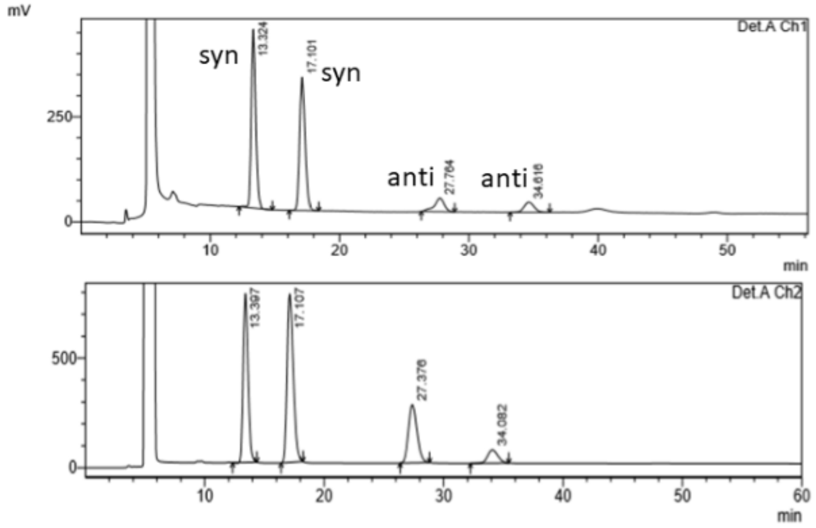

(*R*)-4-hydroxy-4-(4-nitrophenyl)butan-2-one[2, 3]:

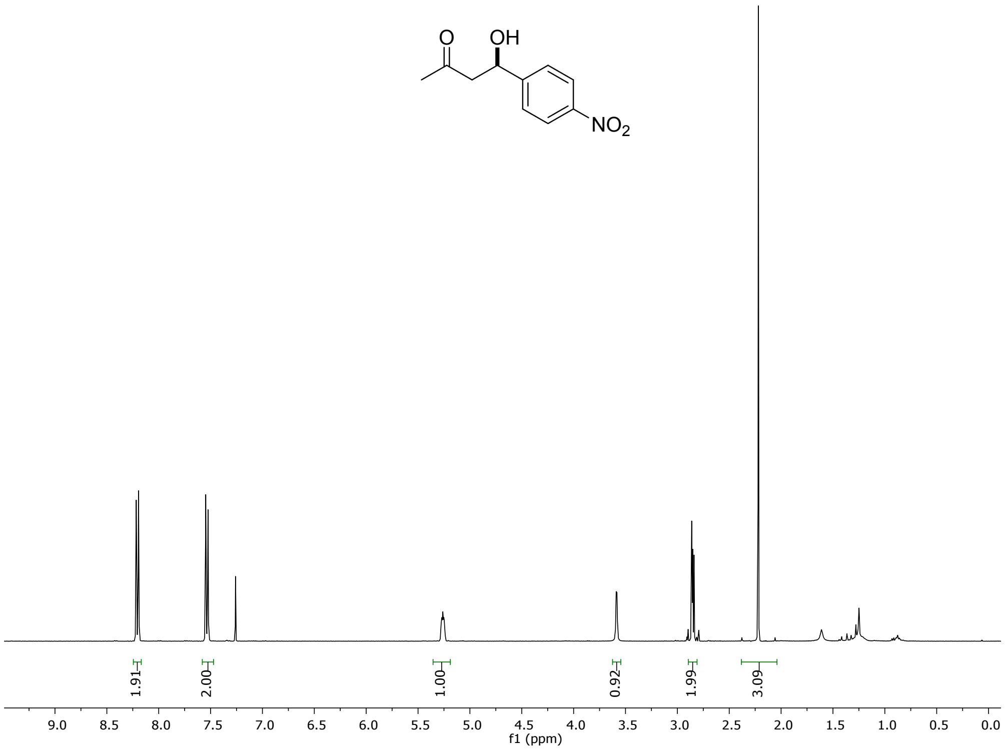

^{1}H NMR (400 MHz, $CDCl_3$) δ (ppm) 8.21 (d, *J* = 8.8 Hz, 2H), 7.52 (d, *J* = 8.5 Hz, 2H), 5.24 (dd, *J* = 7.0, 5.3 Hz, 1H), 3.59 (s, 1H), 2.84 (m, 2H), 2.20 (s, 3H).
Chiral analysis was performed using a Chiralpak ID column eluting with n-hexane / isopropanol (90/10) mobile phase, flow 1 mL/min.

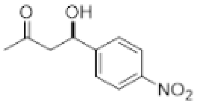

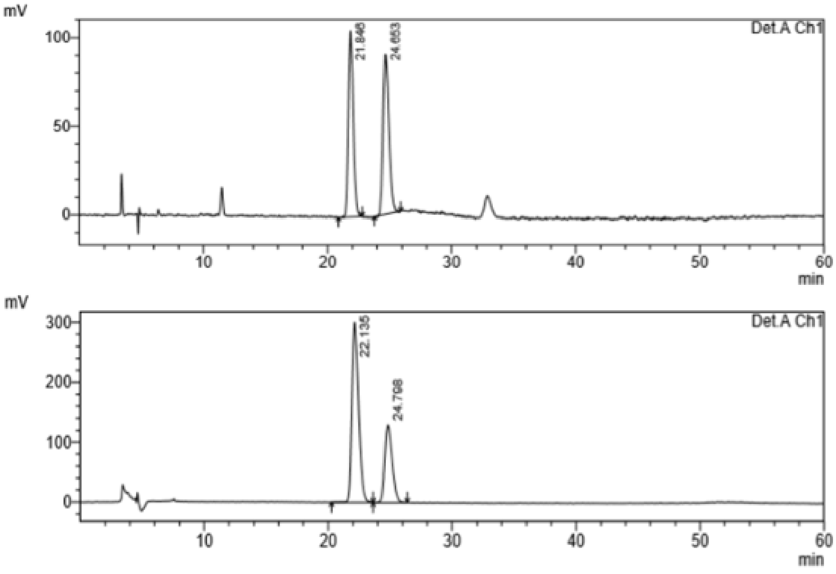

(S)-2-((R)-(4-chlorophenyl)(hydroxy)methyl)cyclohexan-1-one:

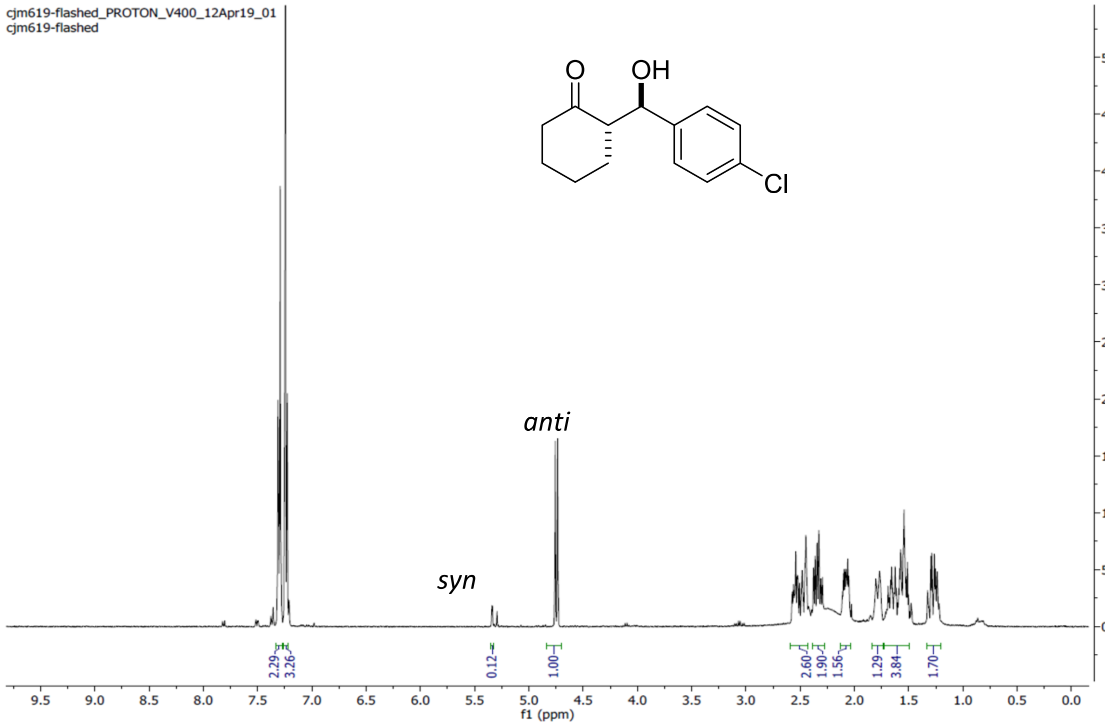

^{1}H NMR (400 MHz, $CDCl_3$) δ (ppm) 7.30 (d, *J* = 8.5 Hz, 2H), 7.24 (d, *J* = 8.5 Hz, 2H), 4.75 (d, *J* = 8.7 Hz, 1H), 2.57-2.44 (m, 2H), 2.38-2.29 (m, 1H), 2.08 (m, 1H), 1.78 (m, 1H), 1.69-1.51 (m, 3H), 1.27 (m, 1H).

Chiral analysis was performed using a Chiralpak ID column eluting with n-hexane / isopropanol (97/3) mobile phase, flow 1 mL/min.

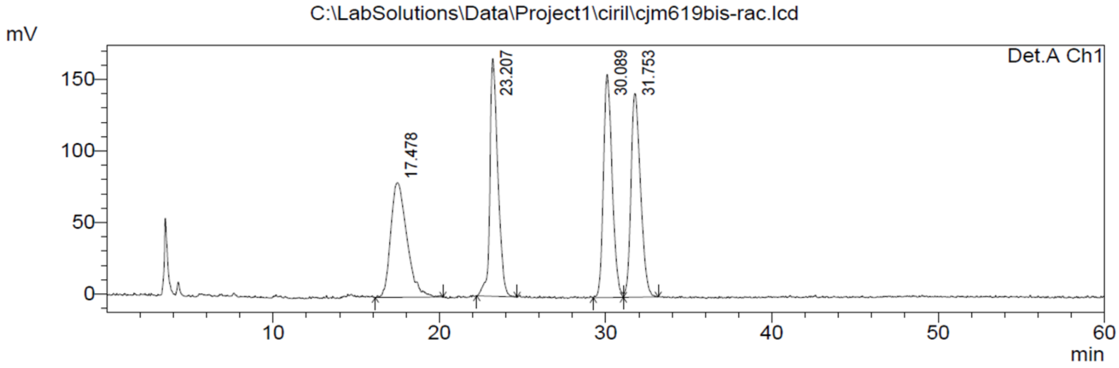

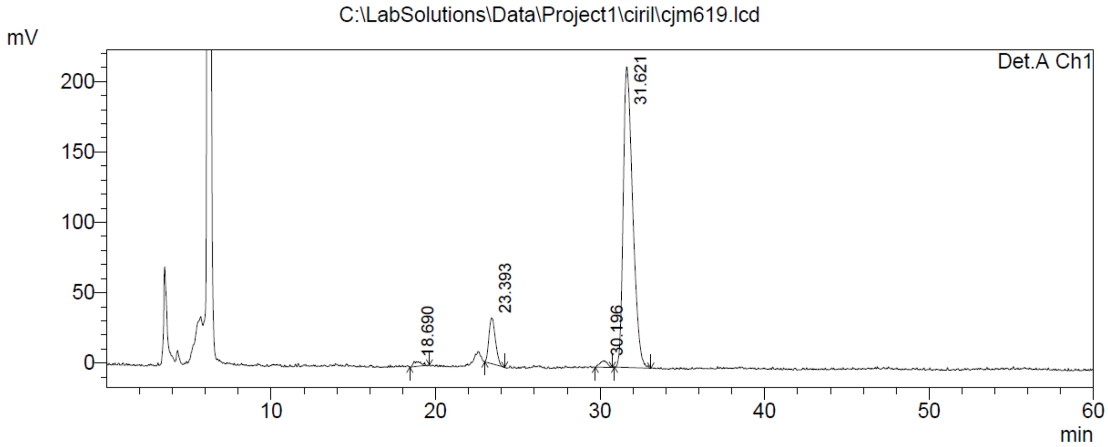

5. Effect of the metal salt in the asymmetric aldol reaction

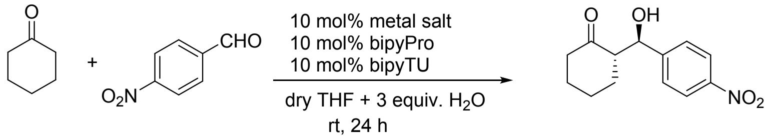

Entry	Metal Salt	Conv. [%][b]	d.r. (*anti/syn*)[b]	ee [%][c]
1[a]	$Zn(OSO_2CF_3)_2$	16	89/11	n.d.
2	$Zn(OSO_2CF_3)_2$	67	81/19	76
3[a]	$Zn(BF_4)_2{\cdot}xH_2O$	57	63/37	60
4	$Zn(BF_4)_2{\cdot}xH_2O$	72	81/19	85
5[a]	$Zn(O_2CCF_3)_2{\cdot}xH_2O$	93	71/29	78
6	$Zn(O_2CCF_3)_2{\cdot}xH_2O$	>99	82/18	91
7[a]	$ZnCl_2$	5	82/18	n.d.
8	$ZnSO_4{\cdot}7H_2O$	8	76/24	n.d.
9	$ZnS_2O_6C_{14}H_{14}$	84	81/19	85
10[a]	$[Cu(CH_3CN)_4]PF_6$	3	83/17	n.d.
11[a]	$[Cu(CH_3CN)_4]BF_4$	6	88/12	n.d.
12	CuCl	33	62/38	84
13	CuBr	21	74/26	77
14	CuI	10	64/36	n.d.
15	$CuCO_3{\cdot}Cu(OH)_2$	18	72/28	n.d.
16	$Cu(ClO_4)_2{\cdot}6H_2O$	20	90/10	96
17	$CuCl_2{\cdot}2H_2O$	10	80/20	77
18	$CuBr_2{\cdot}2H_2O$	16	81/19	85
19	$Cu(CH_3COO)_2$	19	64/36	n.d.
20	$Cu(C_5H_7O_2)_2$	10	62/38	n.d.
21	Ag_2SO_4	62	90/10	88
22	$NiCl_2{\cdot}6H_2O$	0[d]	n.d.	n.d.
23	$CoCl_2{\cdot}6H_2O$	0[d]	n.d.	n.d.
24	$FeSO_4{\cdot}7H_2O$	0[d]	n.d.	n.d.
25	$RuCl_3{\cdot}xH_2O$	16	96/4	n.d.
26	(*p*-cymene)ruthenium(II) chloride dimer (5 mol%)	89	94/6	95

[a] No water added. [b] Determined by ^1H NMR. [c] ee of the *anti* diastereomer. Determined by HPLC on a chiral stationary phase using a Chiralcel OD-H column, n.d., not determined. [d] After 4 hours reacting.

6. Effect of the premixing time of catalyst

A mixture of $Zn(O_2CCF_3)_2.xH_2O$ (2.7 mg, $9.3{\cdot}10^{-3}$ mmol, 10 mol %), bipyPro (2.5 mg, , $9.3{\cdot}10^{-3}$ mmol, 10 mol %) and bipyTU (4.2 mg, , $9.3{\cdot}10^{-3}$ mmol, 10 mol %,) was stirred in dry THF (300 µL) and H_2O (10 µL, 0.55 mmol, 3 equiv. with respect to aldehyde) at room temperature or 0°C at different premixing times. Then, the aldehyde (0.19 mmol) and ketone (1.9 mmol) were added. The reaction was sampled at different hours. Conversion was determined by ^1H NMR ($CDCl_3$) in the crude samples.

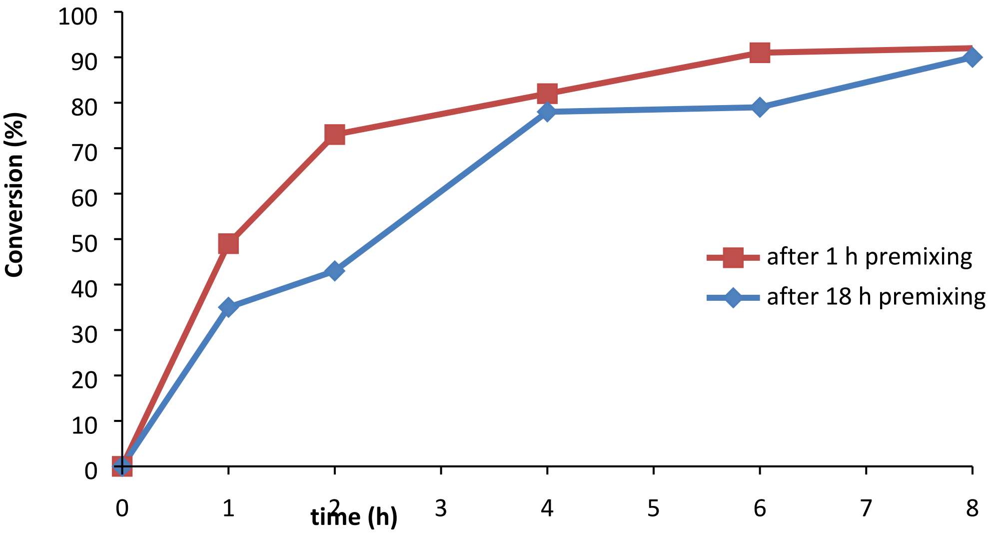

Figure S27. Conversion vs. time plot at different premixing time at room temperature.

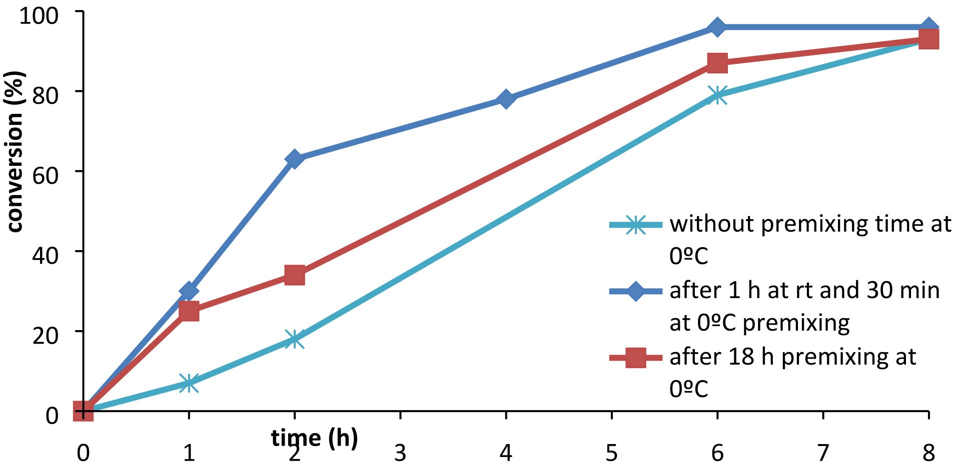

Figure S28. Conversion vs. time plot at different premixing at 0°C.

The results showed that premixing time (1h) at room temperature or at 0°C is necessary to enhance the rate of reaction.

7. Effect of the amount of metal and ligand in the aldol reaction

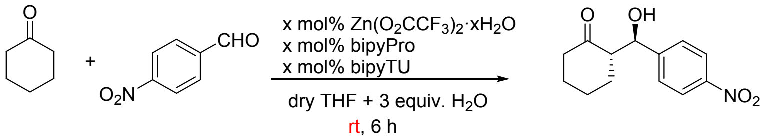

Entry	$Zn(O_2CCF_3)_2{\cdot}xH_2O$ [mol%]	bipyPro [mol%]	bipyTU [mol%]	Conv. [%][a]	dr(*anti/syn*)[a]	ee [%][b]
1	**5**	10	10	81	86/14	93
2	**10**	10	10	91	85/15	91
3	**20**	10	10	79	88/12	92
4	10	10	**15**	92	82/18	96
5	5	5	**10**	67	80/20	86

[a]Determined by ^{1}H NMR. [b]ee of the *anti* diastereomer. Determined by HPLC on a chiral stationary phase using a Chiralcel OD-H column.

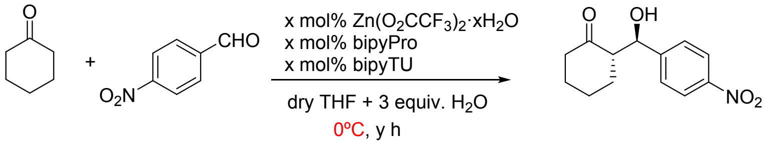

Entry	$Zn(O_2CCF_3)_2{\cdot}xH_2O$ [mol%]	bipyPro [mol%]	bipyTU [mol%]	time [h]	Conv. [%][a]	dr(*anti/syn*)[a]	ee [%][b]
1	10	10	10	6-8	96	92/8	99
2	5	5	5	14	89	91/9	97
3	2	2	2	14	48	89/11	98

[a]Determined by ^{1}H NMR. [b]ee of the *anti* diastereomer. Determined by HPLC on a chiral stationary phase using a Chiralcel OD-H column.

8. ^{1}H NMR Titration of the bipyPro and bipyTU mixture with $Zn(O_2CCF_3)_2$.

Spectra recorded on a Varian 400 MHz spectrometer at room temperature. $CFCl_3$ was added to THF-d_8 to be used as reference signal (δ (ppm) 0.00). ^{1}H NMR and ^{19}F NMR titration experiment was performed by gradual addition of $Zn(O_2CCF_3)_2$ (600 mM) + bipyPro (30 mM) + bipyTU (30 mM) in THF-d_8 to a solution of bipyPro (30 mM) + bipyTU (30 mM) in THF-d_8.

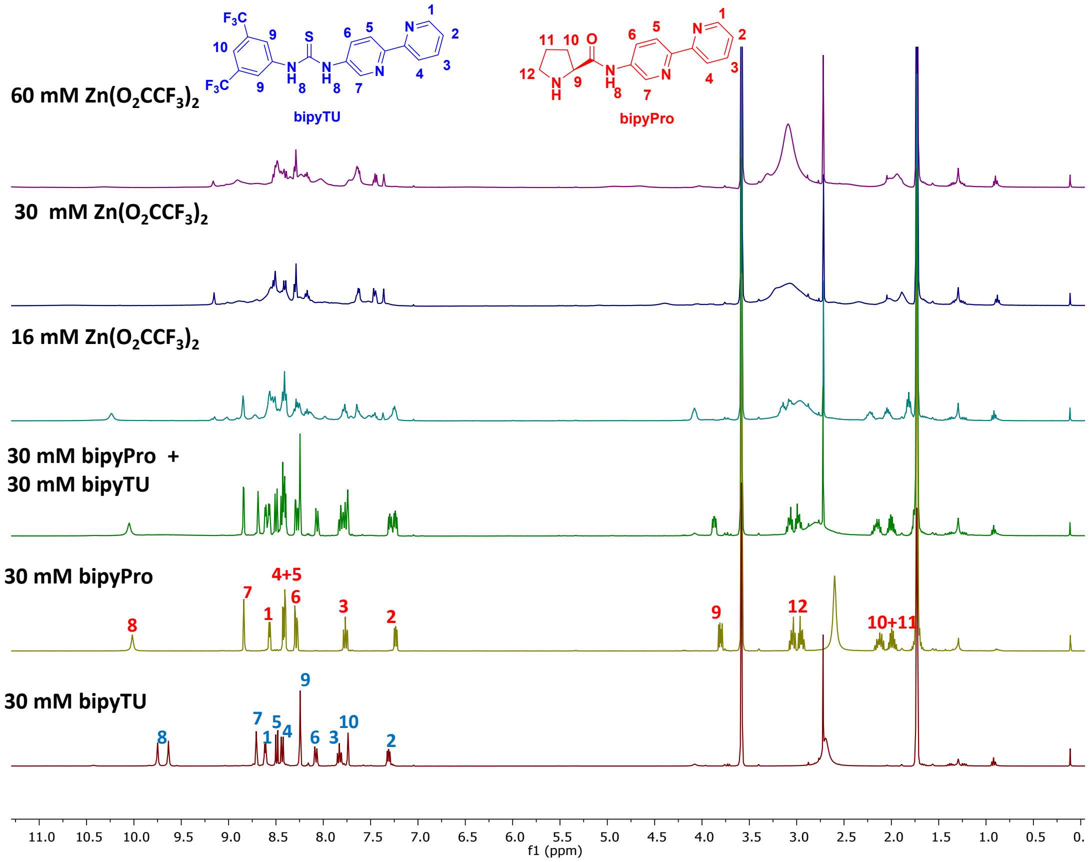

Figure S29. Full scale ^{1}H NMR spectrum.

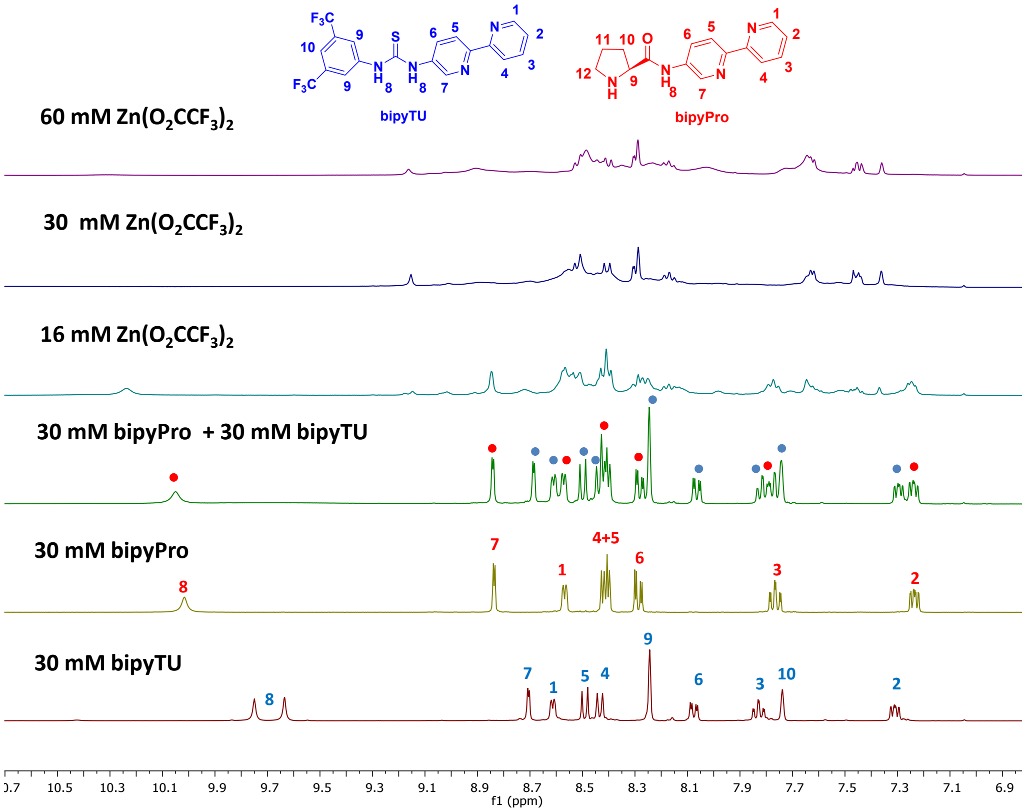

Figure S30. 6.9 – 10.7 ppm expansion of bipyridine, aromatic and H-bonding region.

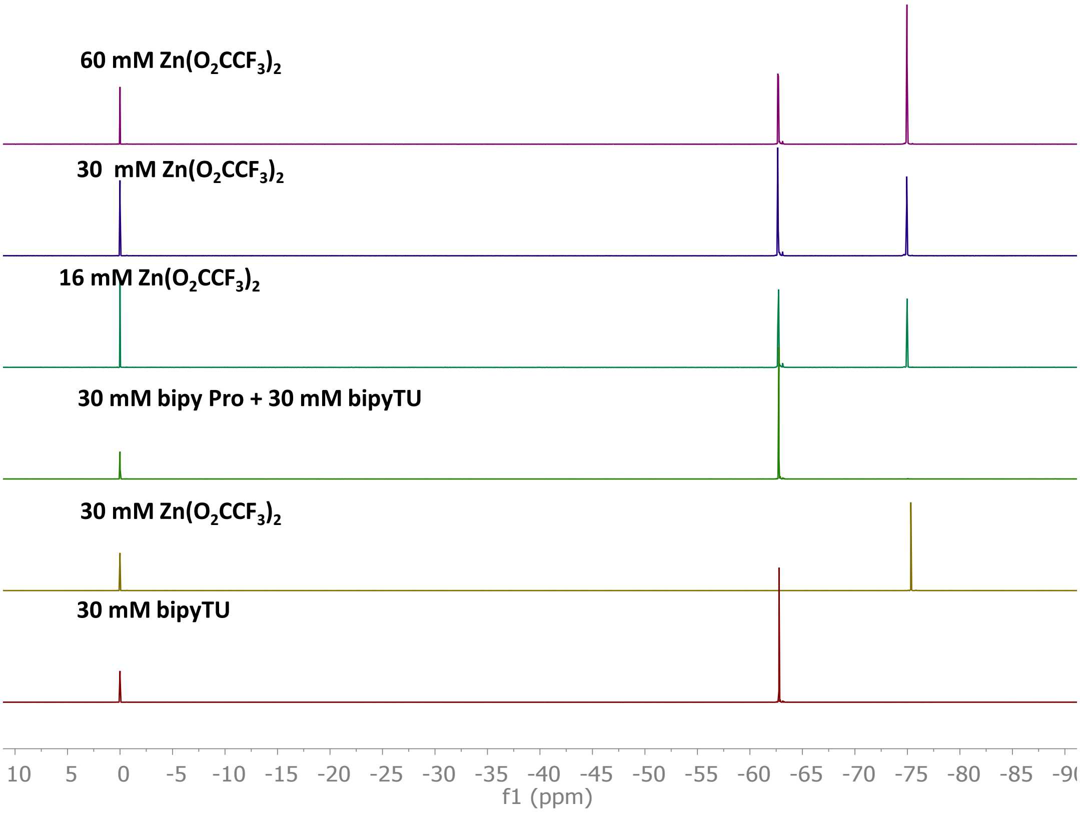

Figure S31. Full scale ^{19}F NMR spectrum. CFCl$_3$ used as reference (0 ppm)

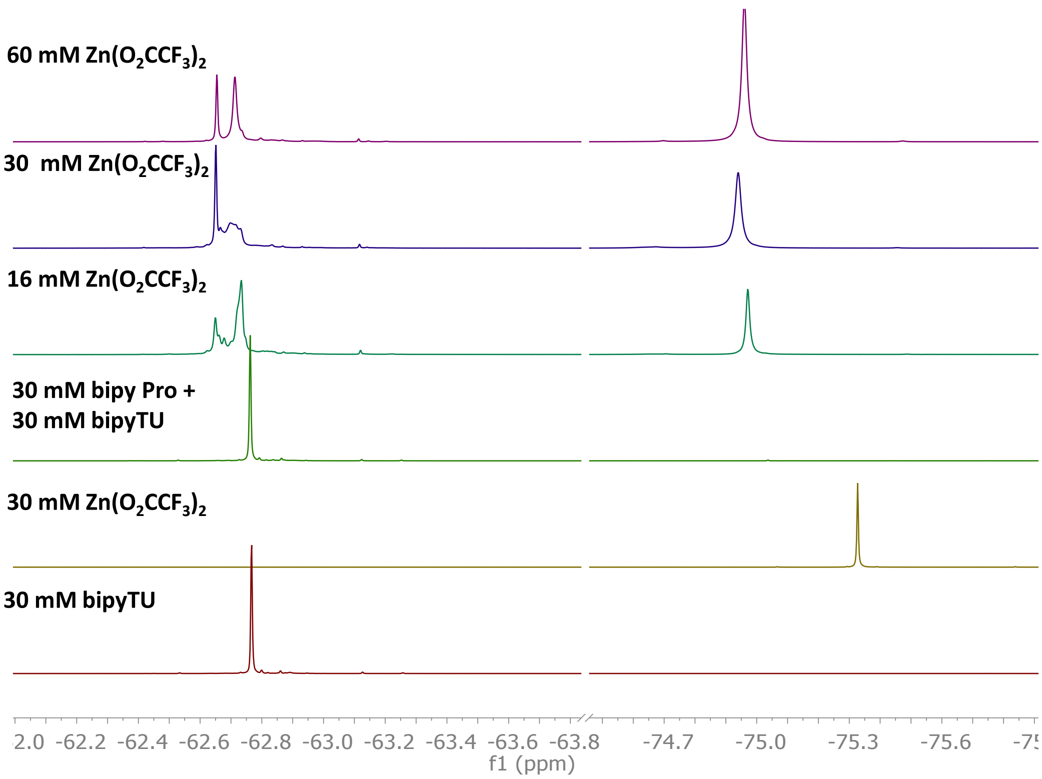

Figure S32. ^{19}F NMR expansion. $CFCl_3$ used as reference (0 ppm).

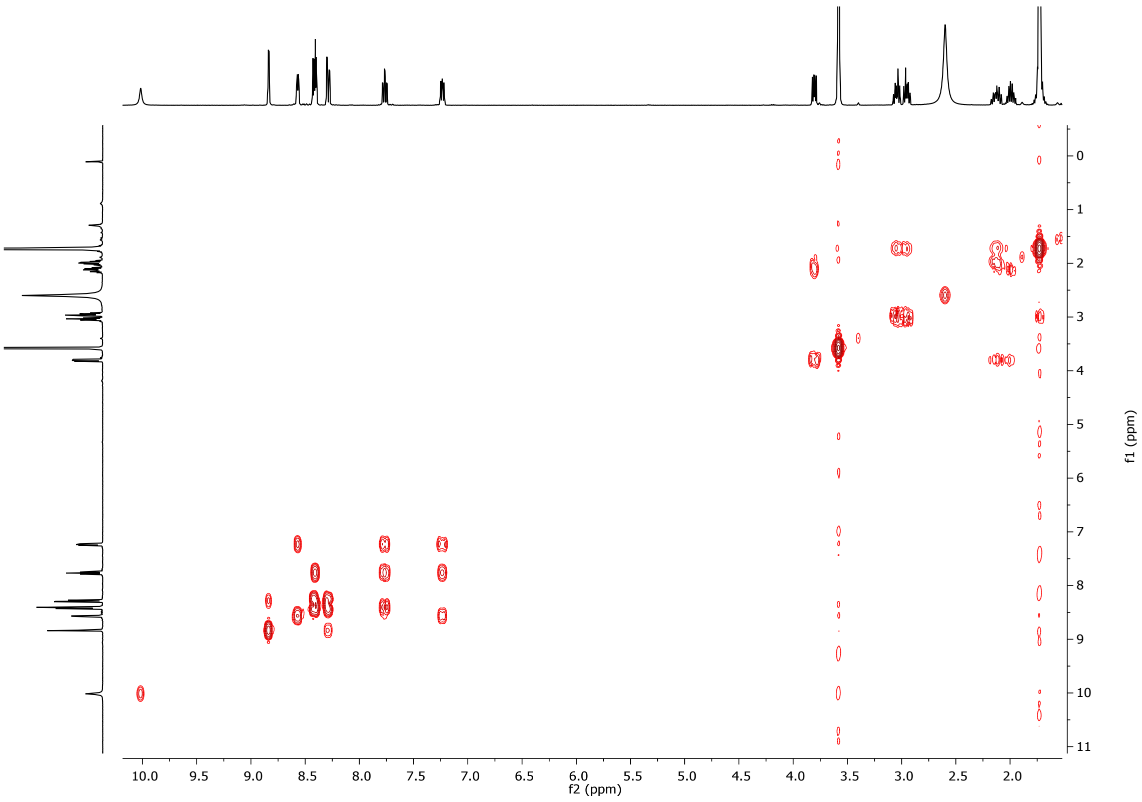

Figure S33. ^1H-^1H gCOSY in THF-d_8 of compound bipyPro.

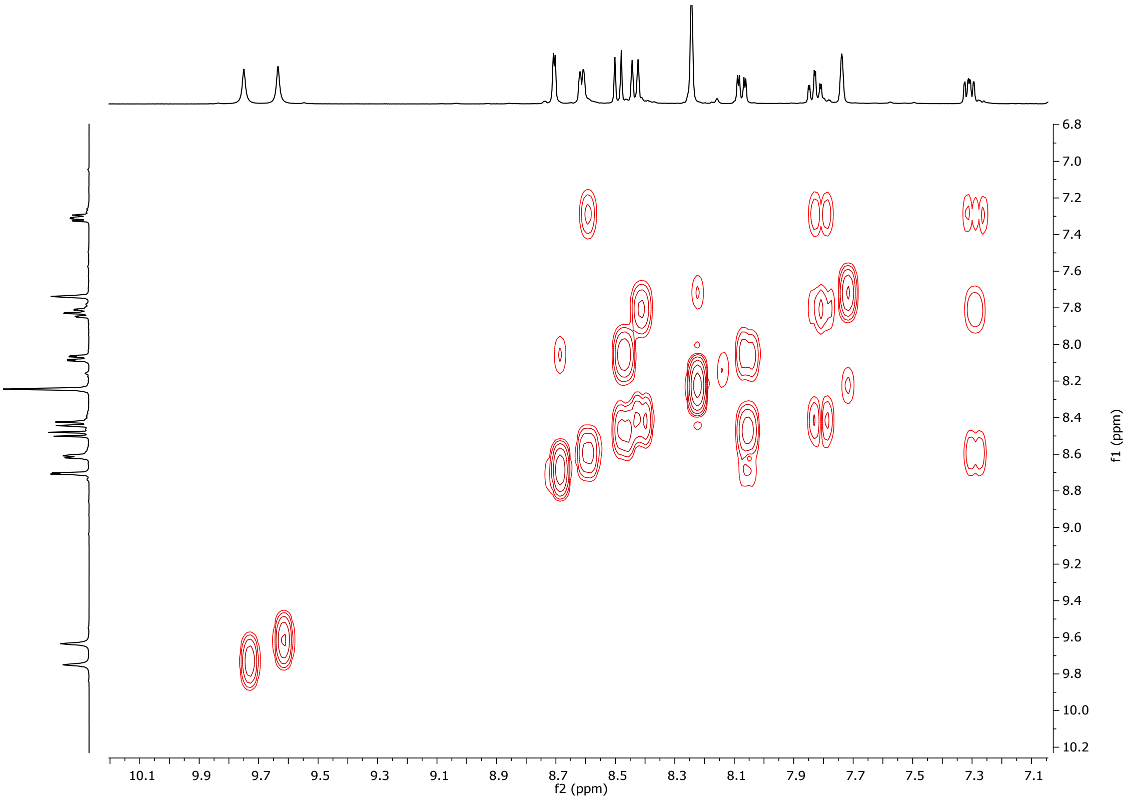

Figure S34. ^1H-^1H gCOSY in THF-d_8 of compound bipyTU.

Broad signals were observed after addition of $Zn(O_2CCF_3)\cdot xH_2O$. It indicates the presence of several species in exchange.

9. Determination of the formation constants

9.1. UV/Vis Titration of the bipyPro with $Zn(O_2CCF_3)_2$.

The stock solution of compound bipyPro (5.22 mM) in THF (spectroscopic grade) was prepared in 1 mL volumetric flasks. 30 µL of this solution was diluted to 5 mL THF (spectroscopic grade) in order to obtain 0.031 mM concentration. The solution in a 10 mm cuvette (2 mL) was then titrated with $Zn(O_2CCF_3)_2{\cdot}xH_2O$ (6.2 mM) + bipyPro (0.031 mM) mixture and UV-vis spectrum was recorded. The resulting data was imported in HypSpec program and fitted to obtain association constants. A total of 9 spectra were used for the refinement in the HypSpec software.[6]

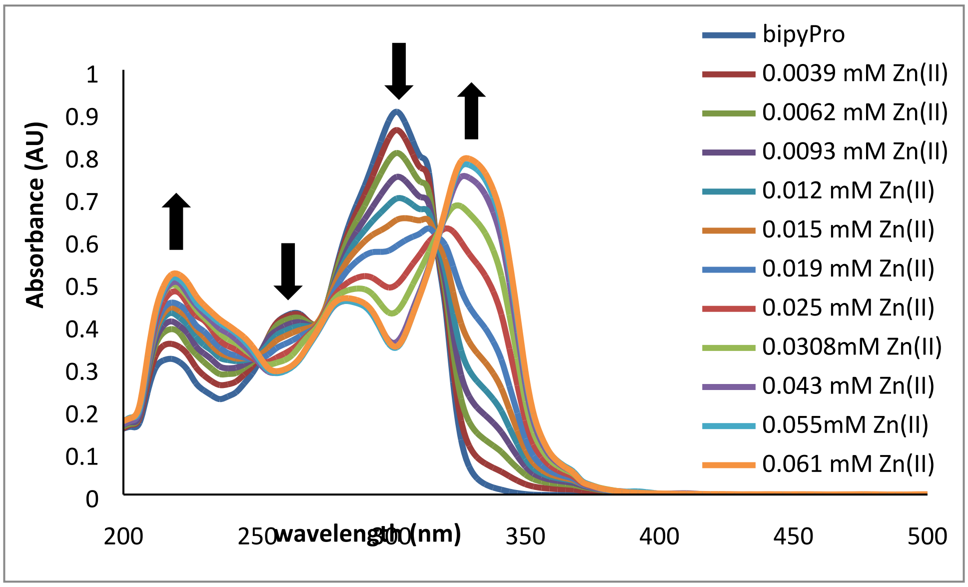

Figure S35. UV/Vis titration of bipyPro upon addition of increasing amounts of $Zn(O_2CCF_3)_2$ (0.0039 mM to 0.061 mM) in THF at 25°C.

The determination of the formation constant was achieved using the model:

$$Zn(O_2CCF_3)_2 + \text{bipyPro} \xrightleftharpoons{K_{MP}} [Zn(\text{bipyPro})]^{2+} + \text{bipyPro} \xrightleftharpoons{K_{MP2}} [Zn(\text{bipyPro})_2]^{2+}$$

		log β (σ)	log K
$[Zn(bipyPro)]^{2+}$	$\log K_{MP} = \log \beta_{MP}$	$\log \beta_{MP} = 6.00$ (0.03)	$\log K_{MP} = 6.00$
$[Zn(bipyPro)_2]^{2+}$	$\log K_{MP} + \log K_{MP2} = \log \beta_{MP2}$	$\log \beta_{MP2} = 10.62$ (0.10)	$\log K_{MP2} = 4.62$

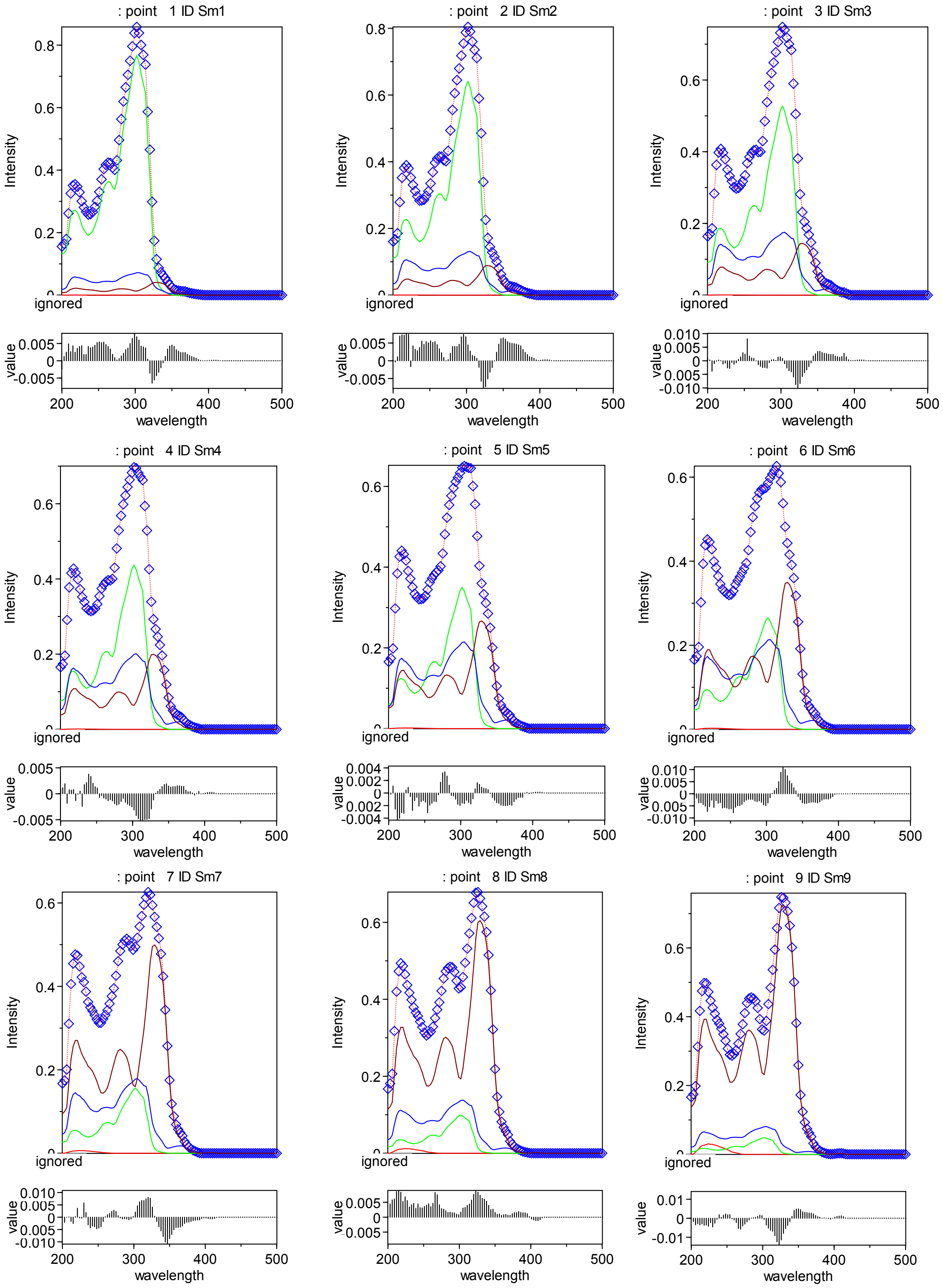

Figure S36. Fitting of experimental data.

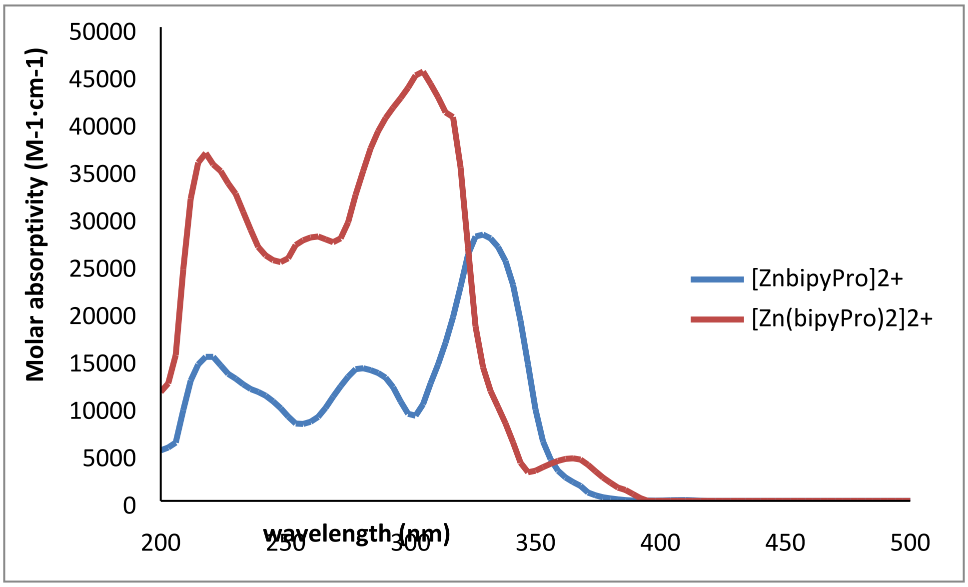

Figure S37. Calculated electronic spectrum of $[Zn(bipyPro)]^{2+}$ and $[Zn(bipyPro)_2]^{2+}$.

9.2. UV/Vis Titration of the bipyTU with $Zn(O_2CCF_3)_2$.

The stock solution of compound bipyTU (5.3 mM) in THF (spectroscopic grade) was prepared in 1 mL volumetric flasks. 30 µL of this solution was diluted to 5 mL THF (spectroscopic grade) in order to obtain 0.032 mM concentration. The solution in a 10 mm cuvette (2 mL) was then titrated with $Zn(O_2CCF_3)_2 \cdot xH_2O$ (5.8 mM) + bipyPro (0.032 mM) mixture and UV-vis spectrum was recorded. The resulting data was imported in HypSpec program and fitted to obtain association constants. A total of 10 spectra were used for the refinement in the HypSpec software.[6]

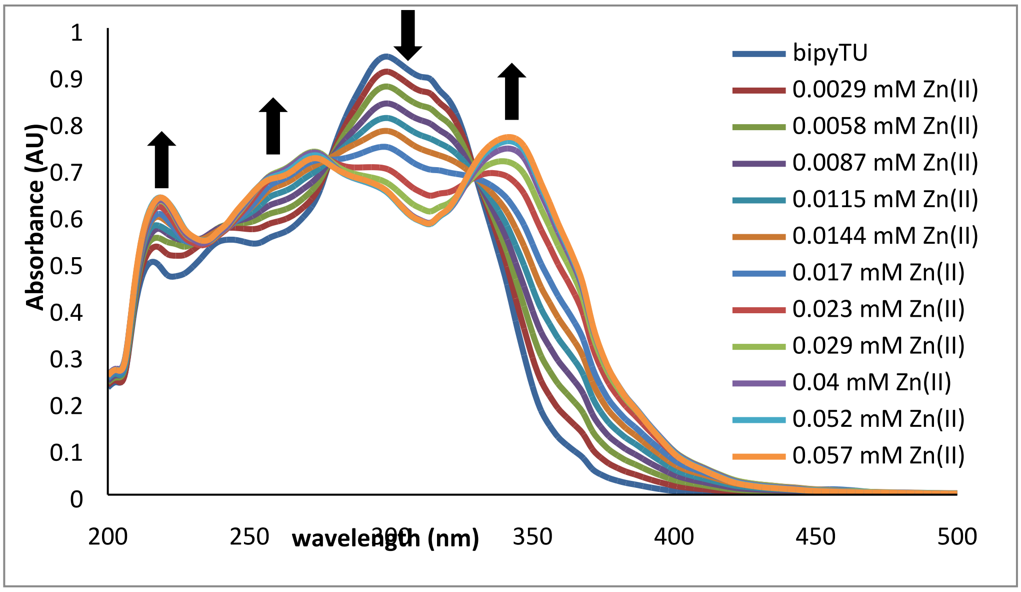

Figure S38. UV/Vis titration of bipyTU upon addition of increasing amounts of $Zn(O_2CCF_3)_2$ (0.0029 mM to 0.057 mM) in THF at 25°C.

The determination of the formation constant was achieved using the model:

$$\mathrm{Zn(O_2CCF_3)_2} + \mathrm{bipyTU} \xrightleftharpoons{K_{MT}} [\mathrm{Zn(bipyTU)}]^{2+} + \mathrm{bipyTU} \xrightleftharpoons{K_{MT2}} [\mathrm{Zn(bipyTU)_2}]^{2+}$$

		log β (σ)	log K
$[\mathrm{Zn(bipyTU)}]^{2+}$	$\log K_{MT} = \log \beta_{MT}$	$\log \beta_{MT} = 6.57$ (0.08)	$\log K_{MT} = 6.57$
$[\mathrm{Zn(bipyTU)_2}]^{2+}$	$\log K_{MT} + \log K_{MT2} = \log \beta_{MT2}$	$\log \beta_{MT2} = 11.04$ (0.25)	$\log K_{MT2} = 4.47$

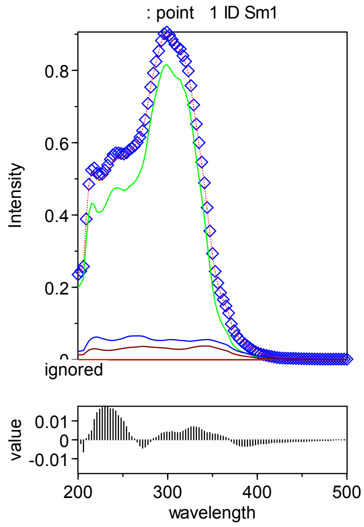

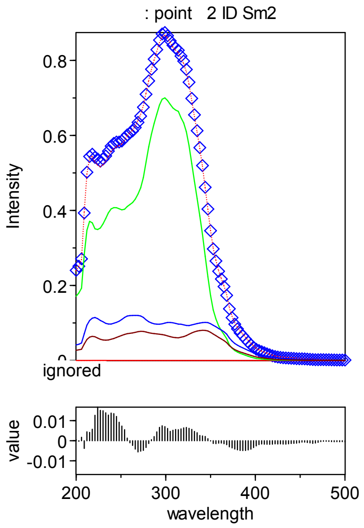

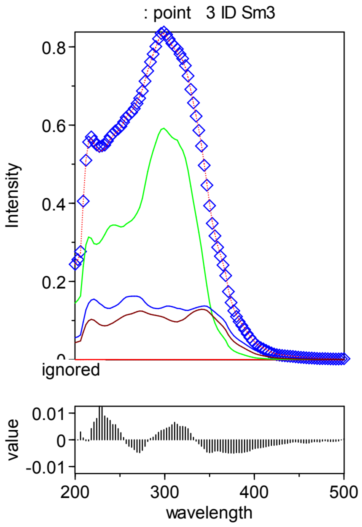

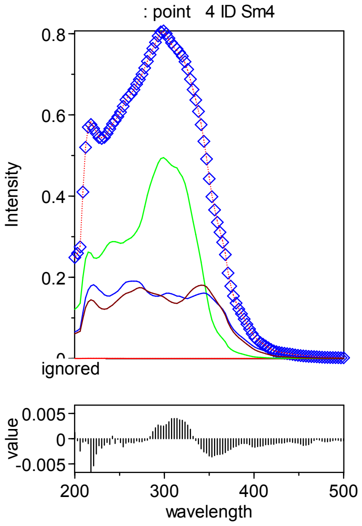

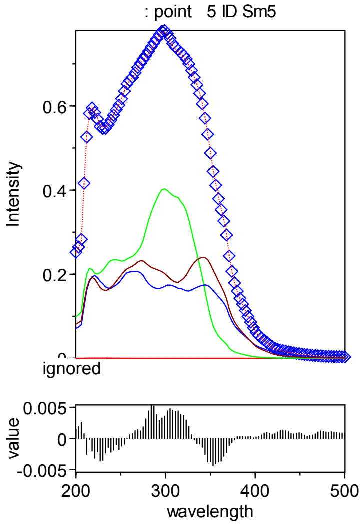

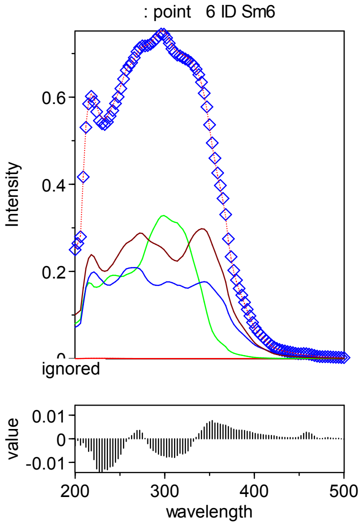

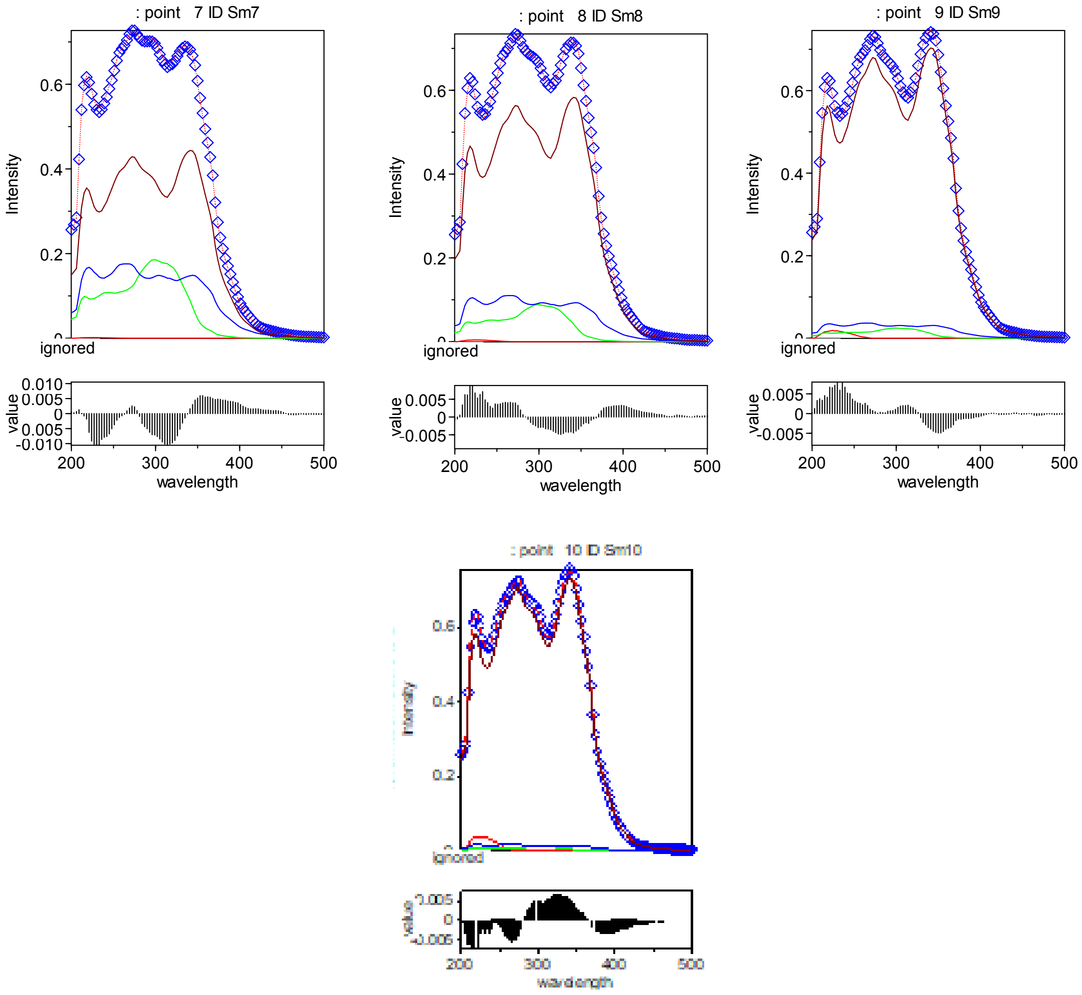

Figure S39. Fitting of experimental data.

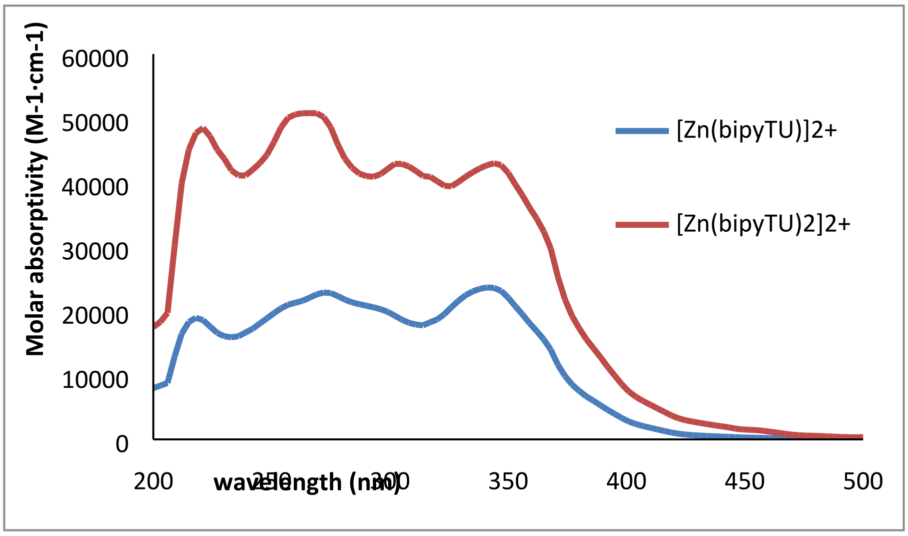

Figure S40. Calculated electronic spectrum of $[Zn(bipyTU)]^{2+}$ and $[Zn(bipyTU)_2]^{2+}$.

9.3. UV/Vis Titration of the bipyPro and bipyTU mixture with $Zn(O_2CCF_3)_2$.

The stock solution of compound bipyTU (4.81 mM) and bipyTU (4.98 mM) in THF (spectroscopic grade) was prepared in 1 mL volumetric flasks. 30 µL of this solution was diluted to 5 mL THF (spectroscopic grade) in order to obtain 0.029 mM and 0.0299 mM concentration, respectively. The solution in a 10 mm cuvette (2 mL) was then titrated with $Zn(O_2CCF_3)_2{\cdot}xH_2O$ (6.86 mM) + bipyPro (0.029 mM) + bipyTU (0.0299 mM) mixture and UV-vis spectrum was recorded. The resulting data was imported in HypSpec program and fitted to obtain association constants. A total of 8 spectra were used for the refinement in the HypSpec software.[6]

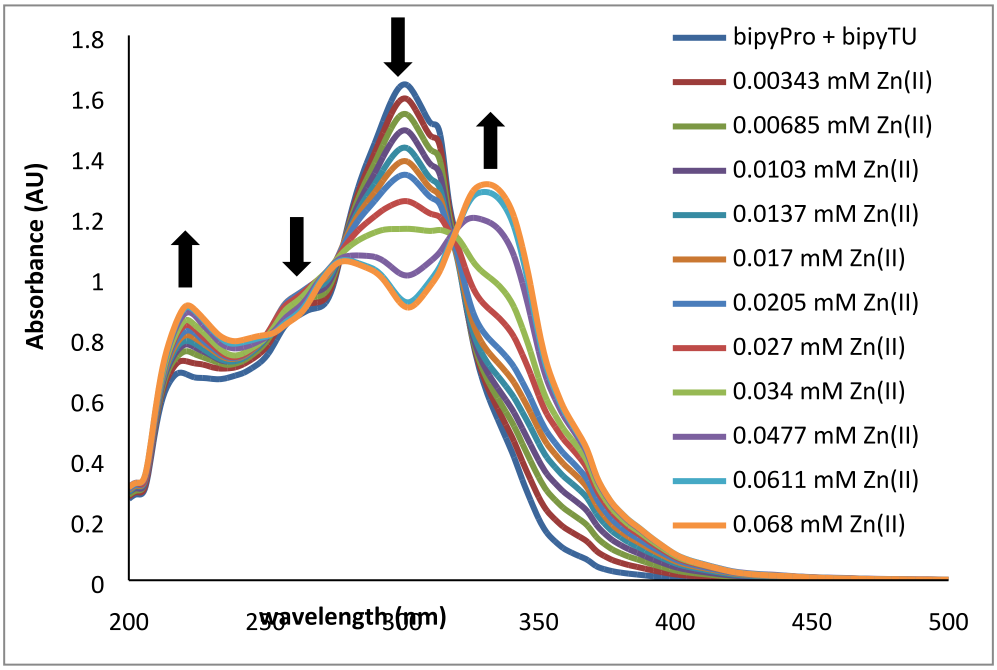

Figure S41. UV/Vis titration of bipyPro upon addition of increasing amounts of $Zn(O_2CCF_3)_2$ (0.0039 mM to 0.061 mM) in THF at 25°C.

The determination of the formation constant was achieved using the model:

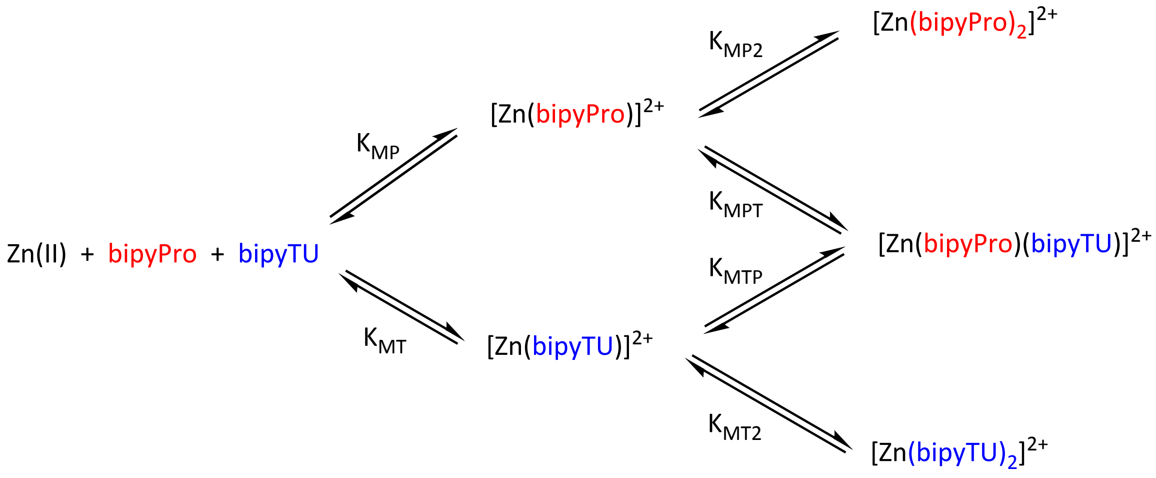

		log β (σ)	log K
$[Zn(bipyPro)(bipyTU)]^{2+}$	$\log K_{MP} + \log K_{MPT} = \log \beta_{MPT}$	$\log \beta_{MPT} = 11.54$ (0.08)	$\log K_{MPT} = 4.97$
$[Zn(bipyTU)(bipyPro)]^{2+}$	$\log K_{MT} + \log K_{MTP} = \log \beta_{MTP}$	$\log \beta_{MTP} = 11.54$ (0.08)	$\log K_{MTP} = 5.54$

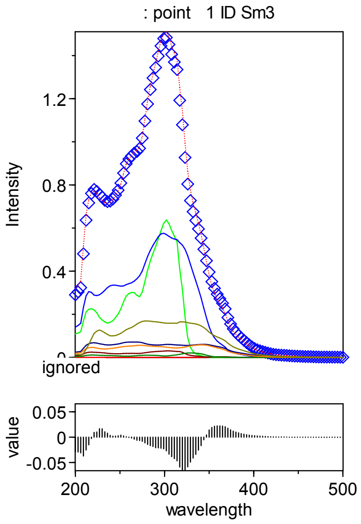

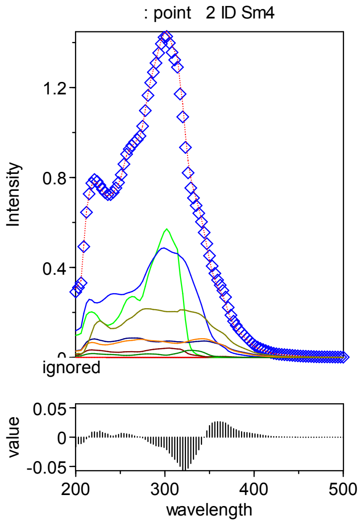

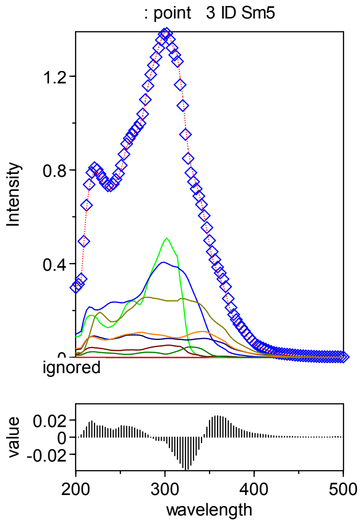

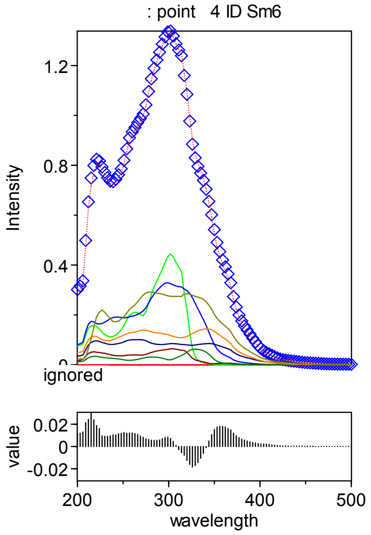

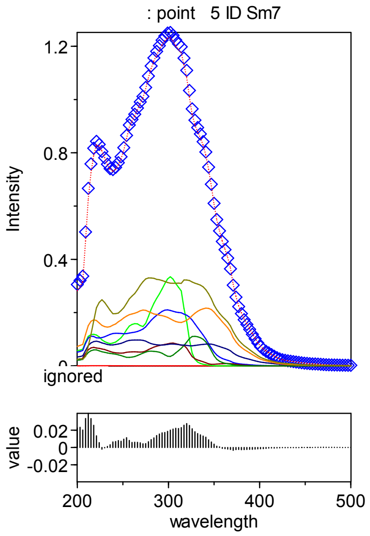

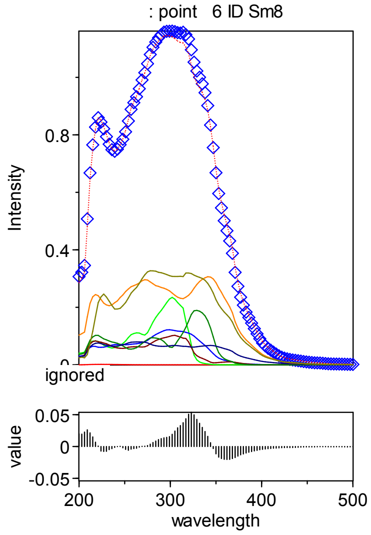

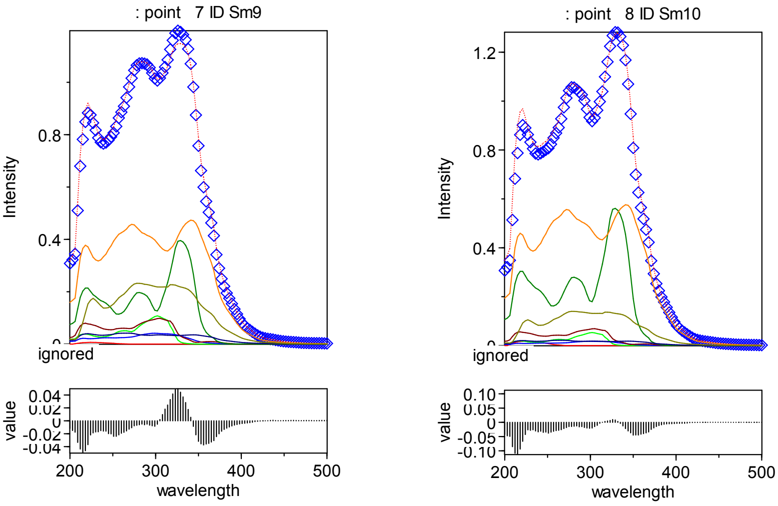

Figure S42. Fitting of experimental data.

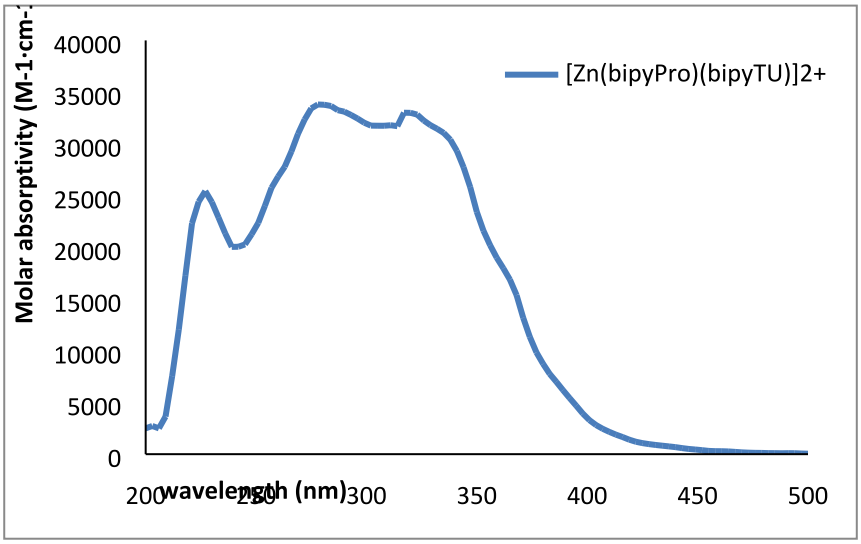

Figure S43. Calculated electronic spectrum of [Zn(bipyPro)(bipyTU)]$^{2+}$.

10. Species distribution of the system

This species distribution diagram was produced by Hyperquad Simulation and Speciation software (HySS).[7]

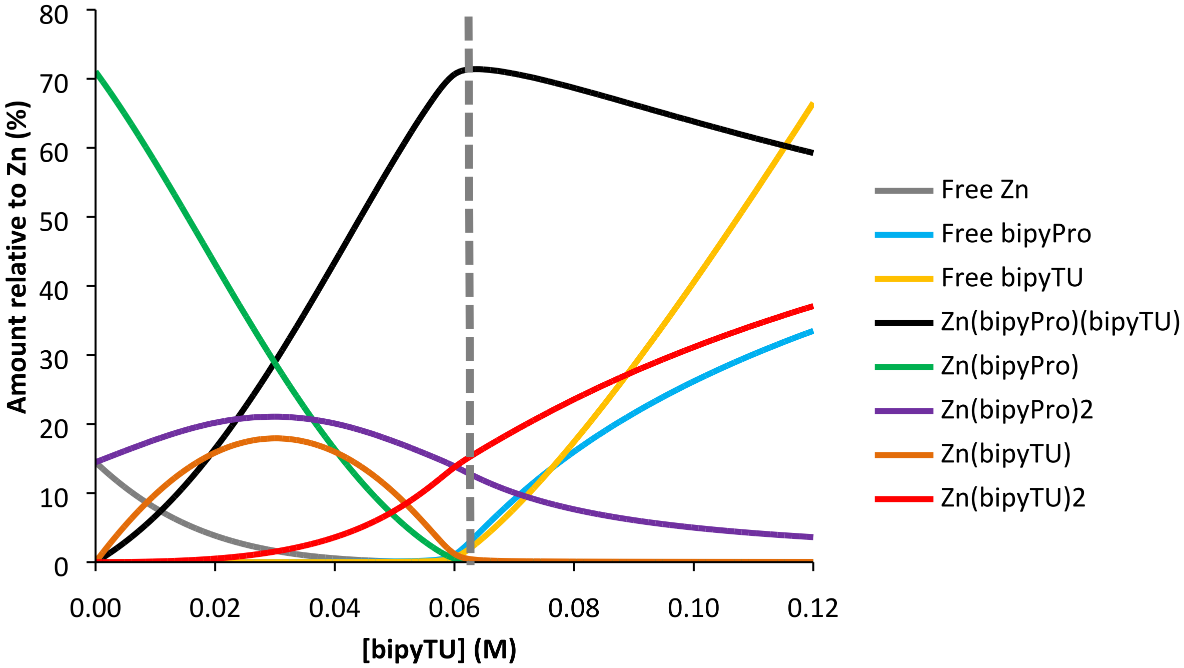

Figure S44. Full species distribution diagram.

11. Mass spectrometry (MALDI-TOF)

MALDI-TOF MS experiments were performed in positive ion mode without matrix. Identified species with the corresponding calculated and recorded isotope distributions are showed.

[Zn(TFA)(bipyPro)]$^+$

found:

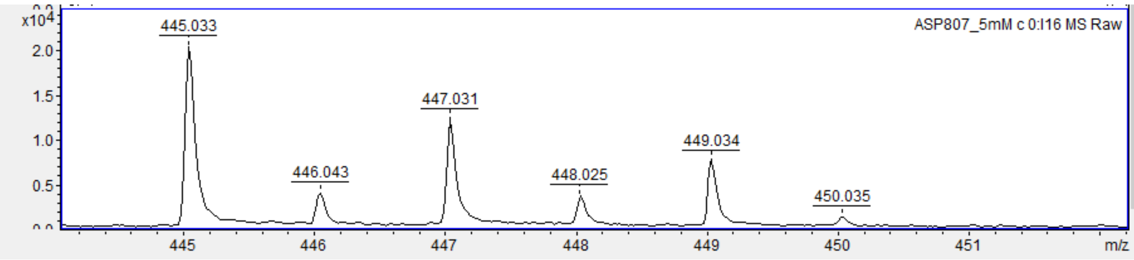

Calculate:

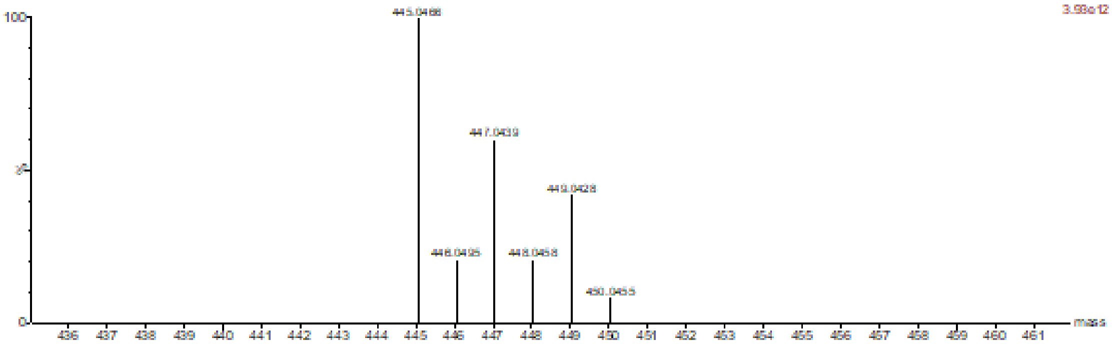

[Zn(TFA)(bipyPro)$_2$]$^+$

Found:

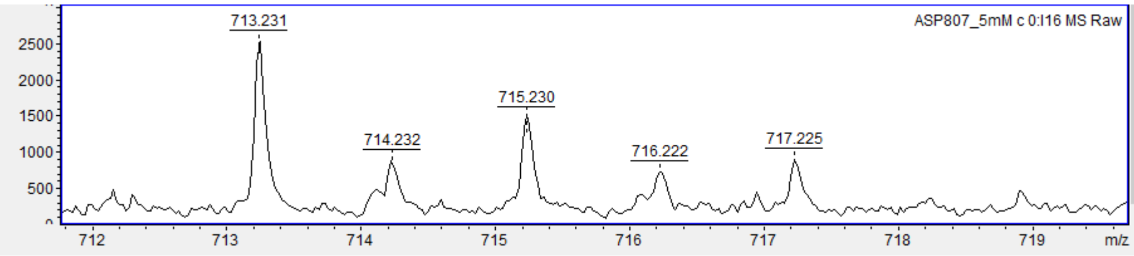

Calculated:

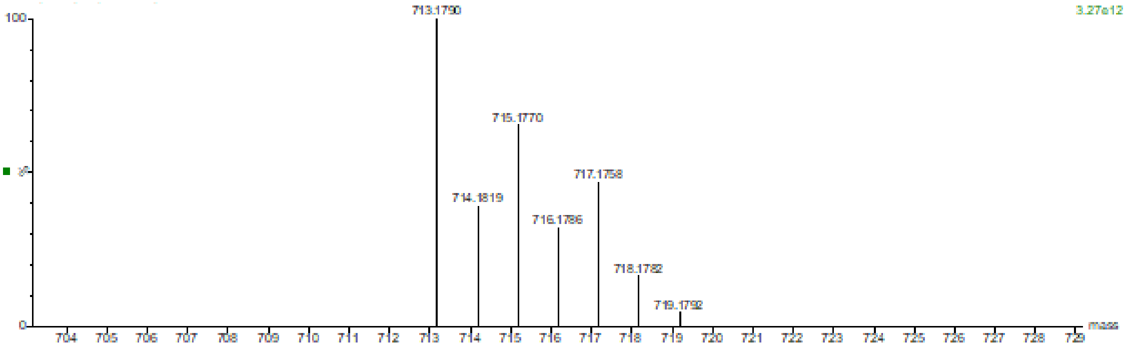

12. Effect of bipyTU on reaction rate

From the conversion vs. time data for the asymmetric aldol reaction between cyclohexanone and p-nitrobenzaldehyde at room temperature, reaction rates were calculated by the Reaction Progress Kinetic Analysis method[8] through exponential fitting followed by its derivative. The plot below can thus be constructed.

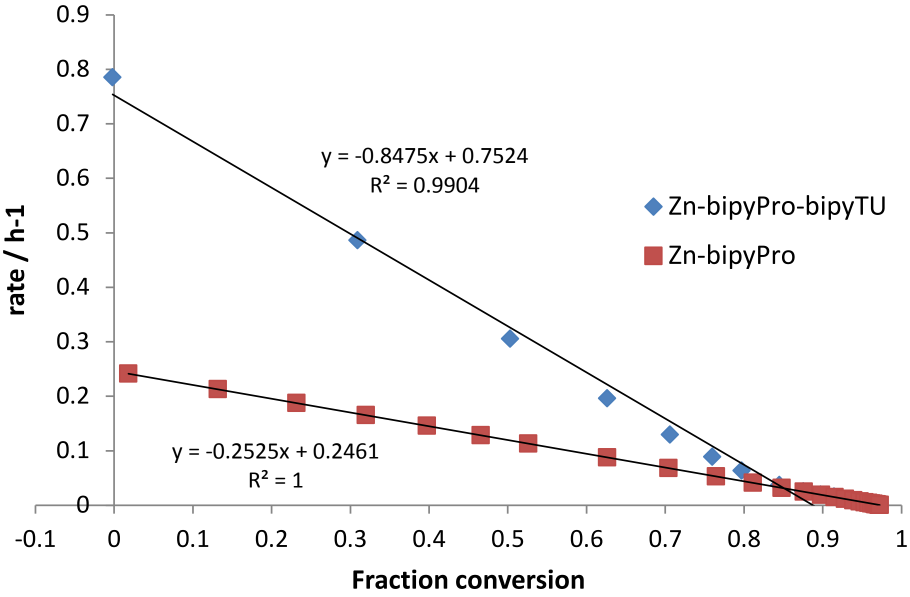

The slopes of the straight lines can be considered as apparent kinetic constants, and their ratio k(Zn-**bipyPro-bipyTU**)/k(Zn-**bipyPro**)=0.848/0.252=3.4 shows more than a three-fold acceleration upon the addition of **bipyTU** to the reaction.

13. Catalyst order in $Zn(O_2CCF_3)_2$+bipyPro+bipyTU:

Conversion *vs.* time was measured by ^1H NMR for several aldol reactions between cyclohexanone and *p*-nitrobenzaldehyde at four different catalyst loadings. Initial rates (slope) were calculated for the initial 2-4 hours:

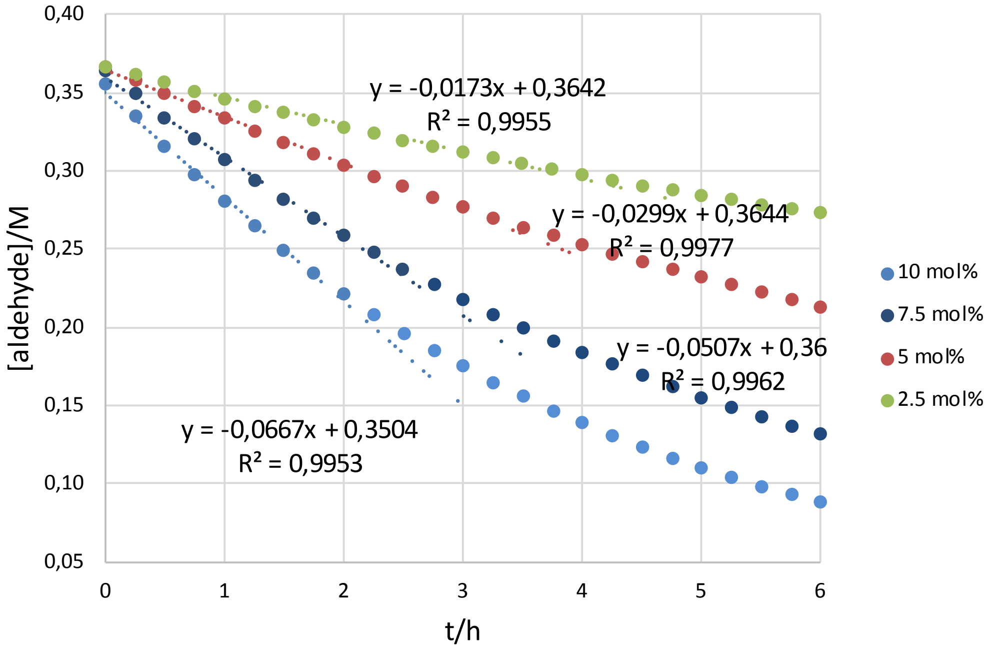

The rate dependence on catalyst concentration was checked:

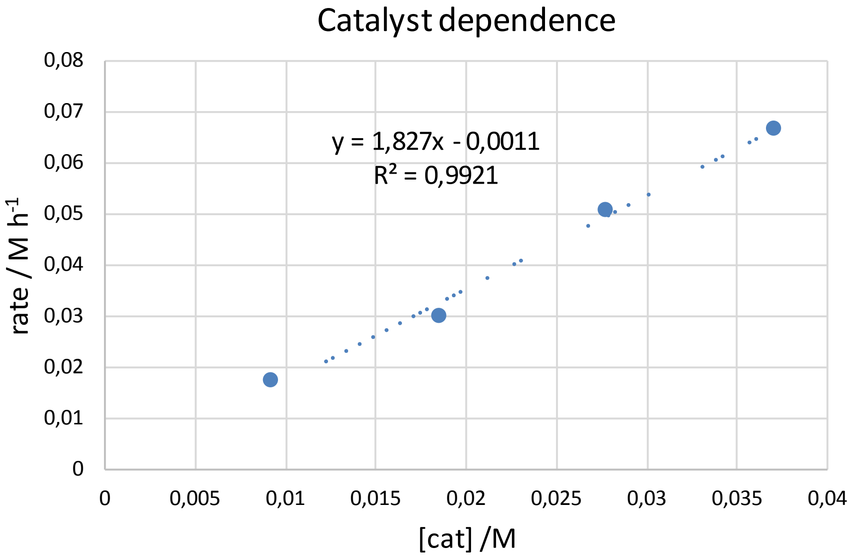

Finally, the catalyst order was determined using a log-log plot:

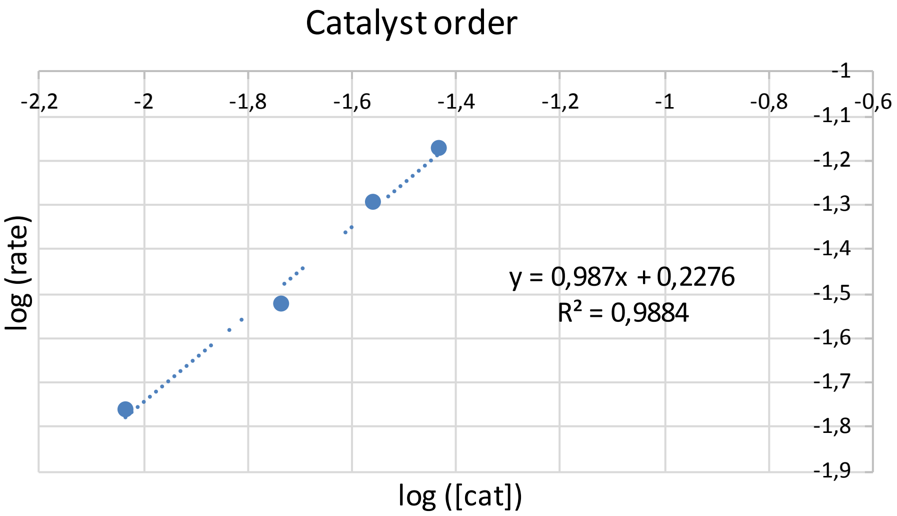

14. Non-linear effects (NLE):

On the reaction between cyclohexanone and *p*-nitrobenzaldehyde.

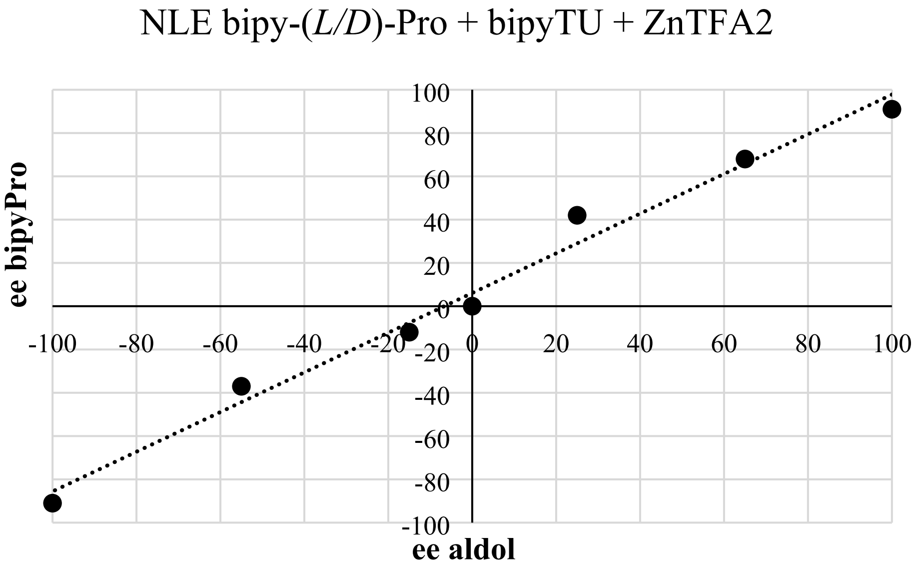

15. Effect of 10 mol% $Zn(O_2CCF_3)_2$ + 20 mol% bipyPro:

To ascertain the possible catalytic activity of $Zn(bipyPro)_2$, the following experiment was performed, which discarded such effect:

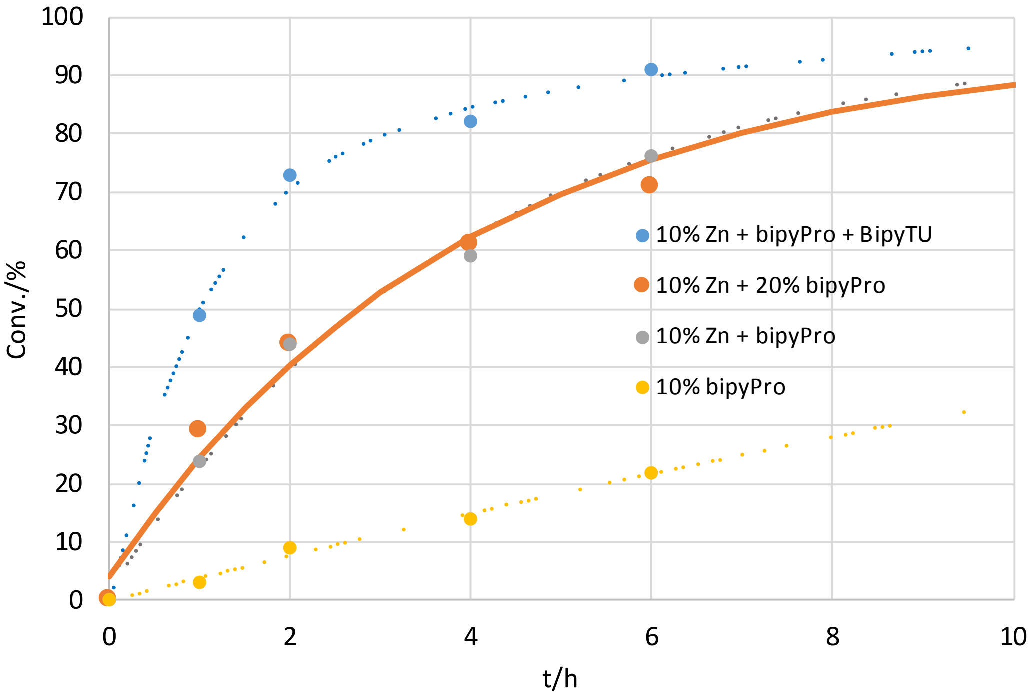

16. References

[1] B. Zhang, R. Breslow, *J. Am. Chem. Soc.* **1997**, *119*, 1676-1681.

[2] A. Serra-Pont, I. Alfonso, C. Jimeno, J. Sola, *Chem. Commun.* **2015**, *51*, 17386-17389.

[3] A. Serra-Pont, I. Alfonso, J. Sola, C. Jimeno, *Org. Biomol. Chem.* **2017**, *15*, 6584-6591.

[4] A. M. Valdivielso, A. Catot, I. Alfonso, C. Jimeno, *RSC Adv.* **2015**, *5*, 62331-62335.

[5] I. Vlasserou, M. Sfetsa, D.-T. Gerokonstantis, C. G. Kokotos, P. Moutevelis-Minakakis, *Tetrahedron* **2018**, *74*, 2338-2349.

[6] P. Gans, A. Sabatini, A. Vacca, *Talanta* **1996**, *43*, 1739-1753.

[7] L. Alderighi, P. Gans, A. Ienco, D. Peters, A. Sabatini, A. Vacca, *Coord. Chem. Rev.* **1999**, *184*, 311-318.

[8] D. G. Blackmond, *Angew. Chem. Int. Ed.* **2005**, *44*, 4302-4320.